



UNIVERSITY OF LEEDS

This is a repository copy of *Advances in native high-performance liquid chromatography and intact mass spectrometry for the characterization of biopharmaceutical products*.

White Rose Research Online URL for this paper:  
<http://eprints.whiterose.ac.uk/123356/>

Version: Accepted Version

---

**Article:**

Tassi, M, De Vos, J, Chatterjee, S et al. (3 more authors) (2018) *Advances in native high-performance liquid chromatography and intact mass spectrometry for the characterization of biopharmaceutical products*. *Journal of Separation Science*, 41 (1). pp. 125-144. ISSN 1615-9306

<https://doi.org/10.1002/jssc.201700988>

---

(c) 2017 WILEY-VCH Verlag GmbH & Co. KGaA, Weinheim. This is the peer reviewed version of the following article: 'Tassi, M., De Vos, J., Chatterjee, S et al. *Advances in native high-performance liquid chromatography and intact mass spectrometry for the characterization of biopharmaceutical products*. *Journal of Separation Science*, 41 (1). pp. 125-144.' Published in final form at <https://doi.org/10.1002/jssc.201700988>. This article may be used for non-commercial purposes in accordance with the Wiley Terms and Conditions for Self-Archiving.

**Reuse**

Items deposited in White Rose Research Online are protected by copyright, with all rights reserved unless indicated otherwise. They may be downloaded and/or printed for private study, or other acts as permitted by national copyright laws. The publisher or other rights holders may allow further reproduction and re-use of the full text version. This is indicated by the licence information on the White Rose Research Online record for the item.

**Takedown**

If you consider content in White Rose Research Online to be in breach of UK law, please notify us by emailing [eprints@whiterose.ac.uk](mailto:eprints@whiterose.ac.uk) including the URL of the record and the reason for the withdrawal request.



[eprints@whiterose.ac.uk](mailto:eprints@whiterose.ac.uk)  
<https://eprints.whiterose.ac.uk/>

1 **Advances in native high-performance liquid chromatography and intact mass**  
2 **spectrometry for the characterization of biopharmaceutical products**

3

4 Marco Tassi<sup>1</sup>, Jelle De Vos<sup>1</sup>, Sneha Chatterjee<sup>2</sup>, Frank Sobott<sup>2,3,4,\*</sup>, Jonathan Bones<sup>5</sup>, Sebastiaan  
5 Eeltink<sup>1,\*</sup>

6

7 <sup>1</sup>Vrije Universiteit Brussel (VUB), Department of Chemical Engineering, Brussels, Belgium

8 <sup>2</sup>Antwerp University, Biomolecular & Analytical Mass Spectrometry, Antwerp, Belgium

9 <sup>3</sup>Astbury Centre for Structural Molecular Biology, University of Leeds, Leeds, UK

10 <sup>4</sup>School of Molecular and Cellular Biology, University of Leeds, Leeds, UK

11 <sup>5</sup>The National Institute for Bioprocessing Research and Training (NIBRT), Dublin, Ireland

12

13 (\*) Corresponding authors

14 Prof. dr. S. Eeltink, Vrije Universiteit Brussel, Pleinlaan 2, B-1050 Brussels, Belgium

15 Tel.: +32 (0)2 629 3324, Fax: +32 (0)2 629 3248, E-mail: [sebastiaan.eeltink@vub.be](mailto:sebastiaan.eeltink@vub.be)

16

and

17 Prof. F. Sobott, University of Leeds, Woodhouse Lane, Leeds LS2 9JT, UK

18 Tel.: +44 (0)113 343 2576, E-mail: [f.sobott@leeds.ac.uk](mailto:f.sobott@leeds.ac.uk)

19

20 **Abstract**

21           The characterization of biotherapeutics represents a major analytical challenge. This  
22 review discusses the current state-of-the-art in analytical technologies to profile biopharma  
23 products under native conditions, i.e., the protein 3D conformation is maintained during liquid-  
24 chromatographic analysis. Native liquid-chromatographic modes that are discussed include  
25 aqueous size-exclusion chromatography, hydrophobic interaction chromatography, and ion-  
26 exchange chromatography. Infusion conditions and the possibilities and limitations to  
27 hyphenate native LC to MS are discussed. Furthermore, the applicability of native liquid-  
28 chromatography methods and intact mass-spectrometry analysis for the characterization of  
29 monoclonal antibodies and antibody-drug conjugates is discussed.

30

31 Keywords: protein therapeutics, bioprocessing, native chromatography methods, intact and  
32 native mass spectrometry, ADC, mAb.

33

## 34 **1 Introduction**

35           The demand for biopharmaceuticals, defined as pharmaceutical products originating  
36 from modern molecular biology methods, is rapidly increasing due to their successful  
37 application in the treatment of various cancers and inflammatory diseases. Currently there are  
38 more than 200 approved drugs available and the global market is expected to soon reach \$278  
39 billion [1,2]. Moreover, it is anticipated that more than 50% of new drug approvals will be  
40 biologics, rising to more than 70% by 2025 [3]. Innovations concerning the development of  
41 novel therapeutic proteins can be categorized into four groups depending on their  
42 pharmacological activity [4]. The first group involves protein therapeutics with enzymatic or  
43 regulatory activity that are prescribed to patients that exhibit protein-related deficiencies [5].  
44 For example, a growth hormone deficiency due the lack of a specific protein that results in  
45 failure to grow at the expected rate. The second group concerns protein therapeutics with a  
46 special targeting activity. Protein therapeutics include peptides and protein derivatives [6],  
47 monoclonal antibodies (mAbs) that interact and interfere with a molecule or organism [7], and  
48 antibody-drug conjugates (ADCs) that act as a vehicle to deliver drugs to a specific biological  
49 site [8]. The third group involves protein vaccines that are used in the protection against  
50 deleterious infectious agents [9]. The fourth class regards protein diagnostic reagents that are  
51 used in clinical decision making [10].

52           mAbs and ADCs represent emerging classes of therapeutic agents. Over the last years  
53 more than 60 antibody derivatives have been approved by regulatory authorities for the  
54 treatment of various diseases including cancer [11], multiple sclerosis [12], rheumatoid arthritis  
55 [13], and asthma [14]. Recombinant monoclonal antibodies (~150 kDa) are composed of two  
56 identical heavy chains and two identical light chains linked by disulfide bridges, yielding a  
57 distinct Y-shape appearance. The part of the antibody which contains the antigen binding site  
58 is called the fragment of antibody binding (Fab). Large-scale production of mAbs mainly occurs

59 in mammals cell cultures using host cells such as Chinese hamster ovary (CHO) cells, mouse  
60 myeloma cells such as NS0 or SP2/0 [14]. Biopharmaceutical proteins of other classes, e.g.,  
61 protein therapeutics with enzymatic or regulatory activity, are mainly produced by  
62 microorganisms such as bacteria and yeasts. Mammalian cells are used for the expression of  
63 glycosylated forms of these molecules such as enzyme replacement therapies due to the  
64 requirement for specific glycan based epitopes, e.g., mannose-6-phosphate, needed for delivery  
65 to the lysosome upon administration. Monoclonal antibodies were traditionally developed and  
66 produced using hybridoma technology, i.e., methods in which hybrid cell lines are cultivated  
67 [15]. These cells combine the ability to produce large amounts of mAbs, derived from the B  
68 lymphocytes of an immunized animal, with the immortality and high rate of reproducibility of  
69 cancer cells, derived from immortalized myeloma cells [16]. More modern approaches for the  
70 development of monoclonal antibodies include the use of techniques such as phage display and  
71 humanized mouse models for target discovery followed by molecular optimization and  
72 expression of the developed mAb using industrial scale CHO cell culture. Antibodies provide  
73 the link between the innate and adaptive immune systems thereby requiring two specific  
74 features for optimal response; 1) high and specific antigen binding as determined by the  
75 complementarity determining regions (CDRs) encoded within the variable regions of the light  
76 and heavy chains and 2) the ability to interact with Fc receptors present on innate immune cells  
77 such as macrophages and monocytes to stimulate the immune response [17,18]. Glycosylation  
78 is the biological process in which the addition of glycans or polysaccharides to the antibody  
79 takes place. Advances in protein engineering, e.g. incorporation of non-natural amino acids,  
80 have facilitated the development of mAb-related products such as site-specific antibody drug  
81 conjugates and bispecific antibodies [19,20]. Antibody-drug conjugates (ADCs) are  
82 biochemotherapeutical agents that combine the specificity of the monoclonal antibody with the  
83 cytotoxic (anti-cancer) drug [21]. ADCs are produced by conjugation of the naked monoclonal

84 antibody with small drugs that exert cytotoxic activity. This class of therapeutics is extremely  
85 promising in cancer treatment, and whereas some are already commercially available, e.g.,  
86 Brentuximab vedotin [22] and adotrastuzumab emtansine [23], many others are under  
87 development and investigation [24]. Bispecific antibodies (bs-mAbs) can interact with two  
88 different antigens at the same time, allowing highly efficient cancer treatment. Also, composite  
89 mixtures of mAbs are being exploited as novel biopharmaceutical products. Bispecific mAbs  
90 and composite mAb mixtures enlarge the molecular complexity of drug candidates, putting  
91 even greater demands on the analytical tools to characterize them [24].

92         Biopharmaceuticals are much more complicated to characterize than traditional small  
93 molecule active pharmaceutical ingredients (API). Regulatory guidelines require the  
94 characterization of the primary sequence, posttranslational modifications (PTMs) and higher  
95 order structures present on these molecules, using methods such as liquid chromatography and  
96 mass spectrometry [25]. These analyses are necessary to ensure that the quality of these  
97 biopharmaceuticals is maintained and to ensure the absence of unwanted PTMs such as non-  
98 human glycosylation epitopes, e.g. galactose alpha 1-3 galactose, or the presence of aggregated  
99 forms of the drug product and sub visible particles that may be potentially immunogenic  
100 [26,27]. Chromatographic techniques such as size exclusion chromatography, cation exchange  
101 chromatography and hydrophobic interaction chromatography have, for many years, been the  
102 gold standard for the characterization of aggregates and higher order structures, charge variants  
103 and structural variants arising from PTMs such as oxidation, etc [25]. The considerable  
104 advancements in stationary phase technology, combined with the advent of high resolution  
105 mass spectrometry under native conditions represents key advances for the characterization of  
106 biopharmaceuticals [28]. As these recombinant proteins exist and exhibit their pharmacological  
107 functions as structured molecules, LC and MS methods that enable the characterization of these  
108 molecules in their native state are becoming more and more important as although still required

109 and powerful, bottom up approaches such as peptide mapping can often result in the loss of fine  
110 detail that exists on the molecule in its native form [29]. The ability to hyphenate native LC  
111 separation chemistries with high resolution native MS represents an emerging and important  
112 tool that will provide information that will enable the linking of sequence to structure and  
113 potential functional implications [30].

114 The present review aims at providing a comprehensive overview on native LC  
115 workflows and native MS strategies applied for the characterization of biopharmaceutical  
116 products. Different native LC separation modes, including aqueous size-exclusion  
117 chromatography, hydrophobic interaction chromatography, and ion-exchange chromatography  
118 are discussed. Aspects of method optimization are discussed and major applications realized  
119 with the different native LC modes are highlighted. In addition, the application possibilities of  
120 intact MS for the characterization of biopharmaceutical products are discussed and aspects of  
121 hyphenation to native LC are debated.

122

## 123 **2 Native LC modes**

### 124 **2.1 Aqueous size-exclusion chromatography for the analysis of protein aggregates and** 125 **fragments**

126 In aqueous size-exclusion chromatography (SEC), biomacromolecules are separated  
127 based on their difference in hydrodynamic volume, and hence on the difference in accessibility  
128 of proteins to the intra-particle pore volume of the resin (typically varying between 35-41%) in  
129 absence of solute interactions with the stationary-phase surface. The first size-based separation  
130 of biomolecules, i.e., peptides from amino acids, was reported by Lindqvist and Storgards in  
131 1955 using a column packed with starch [31]. The premier application area of aqueous ~~size-~~  
132 ~~exclusion chromatography~~SEC with respect to the characterization of therapeutic proteins is

133 the quantitative determination of protein aggregation. Information on the molecular mass of  
134 monomeric proteins, possible aggregates or protein fragments is typically obtained based on a  
135 calibration curve created using protein standards. The prediction error on molar-mass accuracy  
136 provided in this way is typically around 12% (when applying a flow rate matching the minimum  
137 of the Van Deemter curve) [32]. Table I provides an overview of frequently employed SEC  
138 columns, including particle and pore size of the resins and corresponding application area with  
139 respect to the characterization of biopharmaceutical products.

140       Whereas the selectivity provided by the SEC column is defined by the size of the  
141 intraparticle pore diameter, the efficiency in a SEC separation is (partially) governed by the  
142 particle diameter. SEC is considered a slow and low-resolution technique, especially compared  
143 to current-state-of-the-art reversed-phase (RP-)LC columns. Due to low diffusivity of  
144 macromolecules, the optimum flow rate (corresponding to the minimum plate height in the Van  
145 Deemter curve) is very low, and in practice modern SEC columns are operated in the C-term  
146 region of the Van Deemter curve. Often columns packed with rather large particles (5  $\mu\text{m}$ ) are  
147 being employed, hence relatively long interparticle diffusion distances compromise the  
148 separation efficiency due to resistance to mass transfer effects. De Vos et al. discussed the need  
149 to downscale particle size to maximize resolution while exploiting the current column-pressure  
150 limitations of 20 MPa [32]. Within this pressure range it was demonstrated that SEC separations  
151 could be conducted without compromising the selectivity or altering the protein conformation  
152 by shear effects. Furthermore, it was demonstrated that a factor of 2 in analysis time could be  
153 gained when using 3  $\mu\text{m}$  SEC resins instead of 5  $\mu\text{m}$  particles, and optimizing the column  
154 length-to-particle-diameter ratio, such that the column efficiency was maintained [32]. The  
155 evaluation of SEC columns packed with sub-3 and sub-2- $\mu\text{m}$  particles for the analysis of mAbs  
156 and ADCs was described by Fekete et al showing that an additional gain in time can be achieved  
157 without compromising analysis time [33,34]. The same group also reported the risk of forming



158 on-column aggregates when applying small-particle columns under high-pressure conditions  
159 [35]. An alternative approach for method speed-up was demonstrated by Diederich et al. who  
160 reported on a sub-2-minute minute method for mAb aggregate analysis using a parallel  
161 interlaced SEC [36], following an approach described by Farnan et al. [37].

162         Derivatized porous silica has become the gold standard stationary-phase resin for SEC  
163 columns applied to biomacromolecule analysis. To reduce strong ionic interactions induced by  
164 acidic surface-silanol moieties, different surface procedures have been investigated. Diol-  
165 modified silica particles have emerged as current state-of-the-art, reducing ionic interactions  
166 and yielding minimal secondary hydrophobic interactions. In 2010, SEC columns packed with  
167 porous hybrid organic/inorganic particulate material modified with diol chemistry became  
168 commercially available, apparently reducing residual surface silanol activity, improving pH  
169 stability, and increasing the mechanical strength and pressure rating of the columns [38,39]. It  
170 is important to note that the adjustment of the mobile-phase pH (between pH 5.5 and 8.5) and  
171 ionic strength (< 100 mM) is still required to counteract all interactions with residual silanol  
172 moieties. Kopaciewicz and Regnier reported on the effects of mobile phase pH and ionic  
173 strength on non-ideal protein elution behavior [40]. Applying low ionic strength mobile phases  
174 (< 100 mM phosphate buffer), electrostatic interactions may affect protein retention. At salt  
175 concentrations > 500 mM, hydrophobic interaction effects may occur, see also discussion in  
176 ‘Section 2.2’. Furthermore, the extent of these interactions was determined to be protein  
177 specific. Ricker and Sandoval validated these findings for the SEC analysis of mouse myeloma  
178 antibodies of similar molecular weight but of varying overall charge [41]. For weakly basic  
179 antibodies, good peak shapes and retention-time accuracies were observed applying mobile-  
180 phase ionic strengths between 50 and 400 mM phosphate buffer pH 7. At ionic strengths > 600  
181 mM peak broadening occurred and the retention time increased due to hydrophobic interactions.  
182 For a strongly basic antibody an ionic strength of 200 mM was found to be optimal for the SEC

183 analysis, with respect to retention time and peak shape. Reducing the ionic strength led to  
184 increased retention times due to electrostatic interactions. At a concentration of 400 mM and  
185 higher, peak broadening was observed and ultimately the peak profile shifted to higher  
186 retention-time values due to hydrophobic-interaction effects affecting the size-based separation.  
187 The effect of sodium and potassium additives on protein aggregation was investigated by  
188 Goyon et al. [42]. When comparing the ratios between high-molecular species and monomers  
189 for a large number of different mAbs and ADCs, no systematic trend in aggregation level was  
190 detected. Experiments showed that the addition of sodium or potassium to the mobile phase  
191 may, to a certain extent, affect the aggregation level, but this is likely a protein-specific effect  
192 [43].

193 Another factor found to critically affect the SEC performance is the pH of the mobile  
194 phase, since pH affects the equilibrium between charged and uncharged forms of functional  
195 groups on both the column resin and the proteins, the latter determined by the pI, typically  
196 varying between 4 and 9 for antibodies [44]. Ricker et al. also conducted SEC experiments for  
197 mAbs applying a mobile phase with a pH-range between 7.0 and 5.5 [41]. When lowering the  
198 mobile-phase pH, protein retention increased, hence application of higher ionic-strength mobile  
199 phases was required to mediate electrostatic interactions. When applying pH 5.5 and high ionic  
200 strength mobile phases, no peak broadening or shift in retention time were witnessed. At pH  
201 5.5 the antibody became more positively charged (shielded by the higher salt content), which  
202 makes the antibody more polar, reducing its tendency for hydrophobic interactions.

203 During manufacturing and storage of biopharmaceuticals, size variants can arise that  
204 can alter the safety and efficacy of the product. Although ~~size exclusion chromatography (SEC)~~  
205 is known as the chromatographic mode with low efficiency and resolution, it is extremely  
206 powerful to assess aggregation and fragmentation. Figure 1 shows the SEC analysis of a Protein  
207 A purified monoclonal antibody recombinantly expressed in ~~Chinese Hamster Ovarian (CHO)~~

208 cells. This example perfectly illustrates the suitability of the technique in highlighting the  
209 presence of high and low molecular-weight variants. An important quality-control parameter  
210 that needs to be assessed during the production and storage of mAbs is the dissociation pattern  
211 of the hinge polypeptide connecting the fragment antigen binding part to the rest of the  
212 antibody. In a recent paper, Dada et al. correlated hinge fragments measured by SEC with a  
213 complementary Capillary electrophoresis – sodium dodecyl sulfate (CE-SDS)  
214 electropherogram [45]. Another important SEC application is the determination of the  
215 molecular weights of the antibody light and heavy chains. Liu et al. compared the performance  
216 of an optimized SEC methods with that of a gradient RP-LC method [46]. Whereas the retention  
217 time of the intact protein and heavy chain fragment coincided in the RP-LC methods, baseline  
218 resolution could only be achieved between intact antibody, the heavy chain and light chain  
219 fragments with SEC. A SEC method to determine the ratio of free therapeutic mAbs and anti-  
220 drug antibody complexed mAb in the serum of animals was described by Boysen et al. [47].

221 Hyphenation of LC, including aqueous ~~size-exclusion chromatography~~SEC, to MS  
222 detection is desired to obtain accurate mass information. Kükrrer et al. described an off-line  
223 SEC-MS workflow for the analysis of dimer, trimer, and tetramer aggregates of stressed intact  
224 human monoclonal antibody (IgG) [48]. A volatile ammonium acetate buffer system yielded  
225 poor chromatographic separation and mass-spectrometry performance. To overcome this  
226 problem, monomeric and aggregate IgG fractions were collected using SEC, applying a  
227 conventional 0.1 M phosphate buffer at pH 7.2, followed by dialysis of the biomacromolecule  
228 fractions and ESI-TOF MS. Re-analysis of the dialyzed samples by SEC indicated that the  
229 oligomeric state of the different fractions was not measurably affected [48]. Shen et al.  
230 developed an on-line native SEC-MS workflow (which included a flow splitter reducing the  
231 solvent and salt intake prior to ESI) to study the effect of enzyme inhibitors on the protein  
232 quaternary structure [49]. Valliere-Douglas et al. presented a native SEC-based desalting

233 method for analyzing cysteinyl-linked ADCs [50]. They also studied post-desalting dissociation  
234 of the denatured ADC during ESI-ionization by comparing with an orthogonal HIC separation  
235 of the mAbs conjugated with 0-8 drugs [50].

236 Different SEC-ESI-MS approaches have also been developed and applied to the  
237 characterization of biotherapeutics that include the application of organic solvents in their  
238 workflow to advance the ESI spray stability [51-53]. Adding organic modifiers to the mobile  
239 phase is also frequently performed to suppress hydrophobic interactions and reduce peak tailing  
240 when analyzing highly hydrophobic biomacromolecules, such as ADCs [53,54]. It is highly  
241 probable that workflows that include organic solvents affect protein conformation,  
242 biological/enzymatic activity of biomacromolecules, protein-biomolecule interactions, and to  
243 certain extent also aggregation level. Although such workflows may be valuable, providing  
244 insights in the chemical structure, these workflows are not regarded as pure native LC. To  
245 further enhance the flow rate compatibility of SEC with MS detection and reduce the salt intake,  
246 it is mandatory to develop column technology with reduced column i.d. The number of SEC  
247 applications developed using sub 1-mm columns is limited. Rea et al. reported the use of 300  
248  $\mu\text{m}$  i.d. capillary SEC columns for mAb analysis purified from harvested cell culture fluid.  
249 After optimizing the fluidics to minimize system dispersion, picogram sensitivity was achieved  
250 in combination with UV detection [55]. Smoluch et al. applied a 300  $\mu\text{m}$  i.d. column format for  
251 the on-line SEC-ESI-MS analysis of peptides in a mass range of 0.1 – 7 kDa [56].

252 To increase the performance of SEC, different aspects with respect to column  
253 technology and instrumentation need to be addressed. Whereas column-packing procedures for  
254 SEC columns with 5  $\mu\text{m}$  particles have been fully optimized, and columns deliver reduced plate  
255 heights (h) of around 2, columns packed with small particles diameters do not yet reach their  
256 full expected kinetic performance [57]. Hence, column packing techniques to establish SEC  
257 columns need to be advanced. Also, column stability is deemed to be an issue. Recently Farrell

258 et al. demonstrated the long-term stability for a current state-of-the-art SEC column packed  
259 with 5  $\mu\text{m}$  particles allowing for over 1500 consecutive runs, analyzing Bevacizumab  
260 aggregates, see Fig. 2 [58]. Similar experiments are required to demonstrate the robustness and  
261 the applicability of SEC columns packed with small particle diameters in a quality control  
262 environment. To further enhance the kinetic performance, core-shell particles for SEC  
263 separations may represent a good alternative to columns packed with fully-porous particles.  
264 Selectivity will be impaired, but the loss in selectivity will be small since more than 60-75% of  
265 the intraparticle pore volume is maintained. Similar to RP-LC, a gain of roughly 25% in  
266 efficiency can be expected due to improved A-, B, and C-term characteristics [59,60]. Pirok et  
267 al. demonstrated the applicability of core-shell particle technology for ~~size-exclusion~~  
268 ~~chromatographic~~SEC separations of polymers [61]. Columns packed with core-shell particles  
269 displayed outstanding resolution for specific (low-molecular) weight polymer separations.  
270 Furthermore, a gain in analysis speed amounting up to one order of magnitude was  
271 demonstrated.

272 Peak volumes provided by columns packed with sub-3- $\mu\text{m}$  particles and small i.d.  
273 columns are significantly lower than obtained using conventional SEC column technology.  
274 Hence, to preserve the high efficiencies provided by these columns, it is important that the  
275 fluidic path is optimized with respect to extra-column dispersion. System-design requirements  
276 and aspect of tubing configurations influencing the separation performance have been described  
277 in a review by De Vos et al. [62]. The importance of system dispersion affecting high-resolution  
278 SEC separations has been addressed by Goyon et al. [42]. Moreover, when using small particle  
279 columns, thermal heating and possible shear-degradation effects need to be anticipated [63].

280

281 **2.2 Hydrophobic interaction chromatography for profiling differences in surface**  
282 **hydrophobicity**

283 In 1948 Shepard and Tiselius reported on hydrophobic interaction chromatography  
284 (HIC) using the term ‘salting-out chromatography’, observing that biomolecules bind to a  
285 hydrophobic surface material in the presence of salt [64]. Over the last years, HIC has gained  
286 significant importance for the characterization of biotherapeutics, allowing to obtain  
287 complementary information to RP-LC [65]. In contrast to RP-LC, in HIC mode, non-denaturing  
288 LC conditions are applied and hence, protein conformation and biological / enzymatic activity  
289 are maintained during the separation. When proteins are introduced in an aqueous environment,  
290 the protein surface will be shielded by ordered layers of water molecules, preventing  
291 hydrophobic interactions with the stationary phase [66]. During a HIC analysis, salt ions in the  
292 mobile phase lead to exclusion of water molecules from the surface, and the breakdown of the  
293 ordered layer is concomitant with an increase of entropy [67]. This favors the formation of  
294 hydrophobic non-covalent interactions between the hydrophobic patches situated at the proteins  
295 surface and the hydrophobic moieties on the stationary phase, decreasing the free energy.  
296 Protein elution based on difference in hydrophobic surface area is achieved by decreasing the  
297 salt concentration of the mobile phase in time.

298 The number of stationary phases available for HIC separations is relatively limited. This  
299 may be because effects of surface chemistry on protein conformation and hence HIC retention  
300 are still under debate. An overview of frequently used HIC columns and corresponding  
301 biopharma applications is provided in Table II. Conventional columns are packed with 5- $\mu\text{m}$   
302 diameter particles. Typically, HIC resins are less hydrophobic as compared to their counterparts  
303 used in RP-LC. The most common column material used in HIC is either surface-modified  
304 silica or polymeric particles coated with short aliphatic groups, i.e., butyl-, hexyl-, or octyl-  
305 chains [68,69]. Whereas these columns are suitable for the analysis of highly hydrophobic  
306 biomacromolecules, particles functionalized with alkylamide functionalities, polyalkylimide  
307 chemistries, and alkyl ethers are applicable for the analysis of biomolecules with a wide range

308 in hydrophobic surface area, including hydrophilic proteins [69]. It should be noted that  
309 different stationary-phase materials also induce protein specific retention effects [70].

310 HIC is typically performed applying an inverse ammonium sulfate gradient in 50-100  
311 mM phosphate buffer pH 7. Protein retention is strongly affected by the salt concentration and  
312 the type of salt employed. The Hofmeister series, providing information on ions that stabilize  
313 the structure of proteins, has frequently been used to predict protein retention in HIC mode [71].  
314 Soluble compounds that are well hydrated and form hydrogen bonds to water molecules will  
315 exclude water molecules from the protein and resin surface, hence promoting hydrophobic  
316 interactions. Salts that promote the formation of hydrophobic interactions are called  
317 kosmotropic, while salts that do not exhibit this property are called chaotropic [72,73].  
318 However, Arakawa noticed that certain salts, including sodium phosphate and magnesium  
319 chloride, promote hydrophobic interactions regardless of their classification within the  
320 Hofmeister series [74]. Sodium chloride and ammonium acetate salts have been used to replace  
321 ammonium sulfate considering that the elution strength of 1 M ammonium sulfate is equivalent  
322 to ~2.6 M sodium chloride and ~3.3 M ammonium acetate [75]. Typically, kosmotropic salt  
323 systems are compatible with the analysis of hydrophilic biomacromolecules, whereas  
324 chaotropic salt systems are compatible with HIC analysis of hydrophobic proteins. To decrease  
325 retention of highly hydrophobic proteins, organic modifiers, including isopropanol and  
326 acetonitrile, are frequently added to the mobile phase [75]. The Eeltink research group recently  
327 demonstrated that the addition of only 2.5% of isopropanol to the mobile phase may lead to  
328 protein conformational changes, significantly affecting the peak profile [70]. Complementary  
329 differential scanning calorimetry analysis demonstrated that the addition of a small amount of  
330 organic modifier leads to the denaturation of the protein investigated ( $\alpha$ -lactalbumin) [70].

331 Two other parameters that influence the protein retention in HIC mode are the mobile-  
332 phase pH and the column temperature. The impact of pH depends on the isoelectric point of the

333 protein. Good practice is to minimize the shift in pH between the pI of the protein and the pH  
334 of the mobile phase, to prevent possible 3D conformation changes, affecting the level of protein  
335 aggregation, or even induce protein denaturation. The effect of temperature on HIC separations  
336 is still under investigation [76,77]. Generally, it can be affirmed that an increase of temperature  
337 (i.e. column temperature) drives an increase in protein retention. The formation of hydrophobic  
338 interactions is an entropy driven process and the temperature increase favors a decrease in free  
339 energy. On the other hand, the increase of (column) temperature can induce undesired  
340 conformational changes of proteins, and possibly lead to a change in the strength of the  
341 hydrophobic interaction when the surface hydrophobicity is altered [78]. A safe range is  
342 retained to be in the temperature interval between 20°C and 40°C [79].

343 HIC has been successfully applied to characterize mAbs with respect to profiling post-  
344 translational modifications, including monitoring of oxidation variants [80], aspartic-acid  
345 isomerization [81], and domain misfolding [82]. In particular, oxidation of the amino-acids  
346 exposed to the storage environment and micro-heterogeneities in the carboxy terminal chains  
347 are common post-translational modifications that need to be monitored in order to guarantee  
348 the quality of mAbs products. Boyd et al. described the separation of native IgG1 from its  
349 oxidized Trp counterpart [80]. The authors also claimed that the HIC approach allows for  
350 profiling of oxidized methionine and isomerization/deamidation products. A comprehensive  
351 study to characterize mAbs variants resulting from variable N- and C-terminal processing and  
352 stress-induced modifications using HIC technology was performed by Valliere-Douglass et al.  
353 [81]. In this study, the authors also demonstrated the applicability of HIC to separate truncated  
354 antibodies from native species.

355 One of the key HIC applications is the determination of the average load of cytotoxic  
356 drug with respect to the antibody, i.e., the average drug-to-antibody ratio (DAR) of ADCs.  
357 Having information of the average DAR ratio is essential, since this value determines the



358 quantity of cytotoxic drug that will be transported to the targeted tumor cell, defining the  
359 efficacy of the chemotherapeutical distribution. Fig. 3 shows the HIC separation of ADCs  
360 having different payloads [82]. The peaks were assigned using the unmodified antibody for the  
361 zero-drug peak and the absorbance ratio measured at 248 and 280 nm for the other peaks, since  
362 the drug and antibody have distinct absorbance maxima at these wavelengths. The cytotoxic  
363 drugs applied are typically hydrophobic, hence when the payload increases also the HIC  
364 retention time increases and the DAR ratio can be calculated by summation of the individual  
365 peak areas multiplied with their respective drug load divided by the total peaks area. Depending  
366 on the type of mAb (IgG1 or IgG2) used, the DAR varied between 2 and 8 for IgG1 and between  
367 DAR 2 up to 12 for IgG2 [83]. DAR 0 refers to the mAb in which the conjugation with the  
368 cytotoxic drug did not occur, while odd DAR numbers (normally present in neglectable  
369 amounts) refer to ADC in which the conjugation is incomplete. The latter two cases are  
370 considered as impurities in ADC analysis. In the case of ADCs derived from IgG1, different  
371 positional isomers can be present in the DAR 2, DAR 4 and DAR 6 forms. Unfortunately, HIC  
372 has no sensitivity towards positional isomers whereas capillary electrophoresis-SDS-PAGE  
373 [84] and also ion mobility may well have. The characterization of ADCs and their payloads  
374 using comprehensive LC modes has been described in an excellent review by Bobaly et al. [85].

375

### 376 **2.3 Ion-exchange chromatography for the analysis of charge variants**

377 The relevance of ion-exchange chromatography (IEX) in biochemical studies was  
378 demonstrated already in 1949 by Cohn, who performed cation and anion-exchange separations  
379 for a trace-analysis study on the enzymatic formation and degradation of nucleic acids [86]. In  
380 recent years, IEX has been widely applied to monitor product quality and consistency of  
381 biotherapeutics. The separation is based on coulombic interactions between the stationary-  
382 phase surface, containing ionic functional groups, and the charges of the therapeutic protein.

383 Since the disposition of charges at the protein surface depends on the native 3D protein  
384 conformation, proteins having structural diversities can be differentiated by means of IEX. The  
385 net charge of a therapeutic protein is not only determined by the amino-acid residues on the  
386 protein backbone, but also charged glycans are accounting for a portion of the net charge of the  
387 protein. These charges not only affect the structure of the protein, and thus determine the  
388 stability and solubility of the therapeutic product, the charges also affect the binding affinity to  
389 receptors and functional groups of the stationary phase, influencing its biological activity  
390 [87,88]. The versatility of IEX in protein analysis is related to the fact that a wide range of  
391 separation conditions with respect to salt concentrations and pH are applicable. An overview of  
392 frequently used columns for the IEX characterization of biotherapeutics is provided in Table  
393 III. The maximum pressure rating of the current commercially-available material is currently  
394 40 MPa, limiting the application of IEX under UHPLC conditions and thus also its possibility  
395 for method speed-up. The majority of applications is performed using 4.6 or 2.1 mm i.d. column  
396 formats. Rea and Farnan reported on the use of capillary columns formats, i.e., 400  $\mu\text{m}$  i.d.  
397 columns packed with 5  $\mu\text{m}$  pellicular strong cation-exchange particles and 300  $\mu\text{m}$  i.d. columns  
398 packed with 1.7  $\mu\text{m}$  non-porous weak-cation exchange particles for the separation of mAb  
399 charge variants [89].

400 IEX separations can be performed using a salt gradient while keeping the mobile phase  
401 pH constant. This increase in ionic strength of the mobile phase promotes protein elution as the  
402 salt ions compete with the adsorbed protein molecules for the ion-exchange sites on the resin.  
403 Salt gradients provide good resolving power and robustness, but are product specific and time-  
404 consuming to develop. Sodium chloride, usually dissolved in a < 50 mM sodium phosphate  
405 buffer, is the most-employed eluent for separating proteins using salt gradients [90-92]. It is  
406 assumed that NaCl does not affect protein conformation. As the nature of the buffer cation and  
407 anion can affect protein retention and peak widths, the selection of the ideal salt buffer system

408 is very important. [93,94]. The effects of eluent salts on the resolution of protein separation has  
409 been described by Gooding et al., and Regnier et al. [95,96]. Not all charge variants are  
410 generally resolved using a salt gradient in IEX mode, especially the acidic variants [97]. As the  
411 pH is remained constant during the elution process, proteins with the same effective charge will  
412 be eluting with poor resolution. Nevertheless, the potential of CEX for mAb characterization,  
413 applying a shallow gradient of increasing salt concentration (typically 200 mM NaCl) at  
414 constant pH, has been reported in several publications [90,98]. Flattening of the salt gradient  
415 only improves the resolution if the pH of the separation is operated near the pI of the proteins  
416 to be analyzed. As it is demanding in a high-throughput quality control environment of  
417 biopharmaceutical industry to tailor salt systems for individual mAbs, alternative elution  
418 approaches are preferred.

419 Proteins can also be eluted in IEX mode by generating a pH gradient across the column.  
420 Irrespectively of how the pH gradient is formed, two modes of chromatofocusing can be  
421 distinguished, i.e., cation chromatofocusing where the stationary phase exhibits cation-  
422 exchange properties and a gradient running from low to high pH is generated, and anion  
423 chromatofocusing which employs an anion-exchange resin and proteins are eluted by applying  
424 pH gradient going from high to low pH. Generating pH gradients in IEX mode is generally  
425 called chromatofocusing, which is a pressure-driven chromatographic variant of isoelectric  
426 focusing (IEF) elution mechanism coined by Sluyterman and Elgersma [99-101]. Whereas  
427 conventional chromatofocusing using an “internally-generated” pH gradient, gradient  
428 chromatofocusing employs an “externally-generated” pH gradient. In the former variant of this  
429 separation method, the buffer capacity of the stationary phase is used to convert a step change  
430 in pH after applying a mobile-phase of a given pH at the column inlet, while the IEX resin is  
431 pre-adjusted at a different initial pH. In this way, an internally-generated pH gradient is  
432 generated as the packing material will buffer the pH step. This travelling pH wave allows to

433 focus proteins, and releasing them once the pH gradient approaches the pI of the  
434 biomacromolecule. To generate an internal pH-wave, either an immobilized ampholytic buffer  
435 bound to a strong ion exchange resin, or non-interacting buffer species in conjunction with a  
436 weak ion-exchange resin being used [102-104]. The major challenge is to precisely generate  
437 the required pH gradient, while minimizing the ionic strength of the running buffer to reduce  
438 its effect on protein retention. The conventional elution buffers are polyampholytes. These  
439 molecules provide a high buffer capacity covering a broad pH range, but are poorly defined,  
440 and have been reported to interact with both the proteins as with the stationary phase resin  
441 [105]. Alternatively, a combination of equally concentrated buffer species with equally spaced  
442 pKa values in the chosen pH range can be employed. Kröner et al. provided an in-silico  
443 optimization method of buffer compositions, resulting in well-controllable pH gradients with  
444 low ionic strength validated for characterization of more than 20 proteins [106].

445 Alternatively, chromatofocusing can also be performed by applying an externally-  
446 generated pH gradient, i.e., by use of the gradient proportioning system of the LC pump. By  
447 gradually mixing the running buffer with successively greater proportions of an application  
448 buffer, while both buffers are set at different pH, a pH gradient is generated in time prior to  
449 entering the column. At the start of the pH gradient proteins are adsorbed on the column head  
450 and the proteins elute once the incoming pH gradient is slightly below the pI of the protein. The  
451 quality of the separation is thus depending strongly on the solvent-proportioning capabilities of  
452 the LC equipment, as poorly controlled pH gradients can result in co-elution of proteins with  
453 similar pI's. The formation of multi-step or multi-variable slope (non)-linear gradients over a  
454 wide pH range, and a buffer system compatible with both anion- and cation-exchange stationary  
455 phases that allows for an arbitrary start- and end-pH value and pH-range are still not available  
456 for this separation mode [107]. Tsonev and Hirsch developed software that can precisely  
457 perform high-order polynomial fitting of titration curves for a dedicated buffer system, allowing

458 controlled gradient formation of any desired shape and slope [107,108] for both cation- and  
459 anion-exchange separations. Furthermore, the algorithm also allows for software-driven control  
460 of pH gradients that can contain additives such as nonionic detergents, organic modifiers, salts,  
461 etc. Fig. 4 shows the comparison between the optimization of an anion exchange separation of  
462 *E. coli* acetone powders performed using a salt gradient (Fig. 4A), and using a pH gradient (Fig.  
463 4B). The steepness of the salt gradients was decreased, at the expense of analysis time, whereas  
464 for the pH gradient separations only the slope of the gradient between pH 3.5 and 2.4 was  
465 varied, see Fig. 4C. The pH gradient separations are offering the best resolution, especially for  
466 the very acidic proteins present in the complex *E. coli* mixture.

467 IEX has emerged as the standard method for the determination of charge heterogeneity  
468 of monoclonal antibodies. It is important to measure product heterogeneity during the  
469 development and production process of mAbs, as many charge variants can arise due to post-  
470 translational modification or product degradation processes. These modifications processes of  
471 the parent protein include C-terminal lysine variants, N-terminal pyroglutamate formation,  
472 deamidation, glycation, and glycosylation, resulting in a modified isoelectric pH (pI) value of  
473 the mAb [109,110]. Vlasak et al. has written a review on the analysis of charge-related  
474 heterogeneity in monoclonal antibodies [111]. IEX is less preferred to study ADC charge  
475 variants, as the linked cytotoxic drugs are changing the hydrophobic surface of the conjugated  
476 antibody resulting in unwanted secondary interactions with the stationary phase and  
477 consequently a poor resolution separation [112]. Some studies have been performed on  
478 retention time models for IEX separations using salt gradients [113,114] and pH gradients  
479 [115]. Fekete et al. applied a Drylab CEX model for the separation of mAb charge variants  
480 using both salt and pH gradients [116,117].

481 The contribution of various posttranslational modifications to monoclonal antibodies is  
482 diverse, with basic amino acids contributing to an increase in the mAbs pI whilst deamidation

483 of asparagine residues and sialic acid present on N-glycans contribute to a decrease in the mAbs  
484 pI. These different contributors to the overall protein chemistry of the mAb make cation  
485 exchange (CEX) chromatography the analysis method-of-choice to study mAb charge variants.  
486 In CEX mode, the separation of proteins is governed by the surface-charge, charge-distribution,  
487 and the geometry of the protein. CEX separations of mAbs is typically performed by applying  
488 a gradient with increasing salt concentration (i.e. 100-200 mM sodium chloride), while  
489 maintaining the pH of the buffer constant. The pH of the buffer depends on the isoelectric point  
490 of the mAbs under analysis but in general the pH range is between 7.5 and 9 [118]. Separation  
491 of mAbs in anion exchange (AEX) mode, is also being performed, mainly to separate oxidized  
492 variants of mAbs. Teshima et al. showed how AEX was effective in the analysis of three force-  
493 oxidized antibodies as compared to CEX. It was demonstrated that AEX revealed oxidized  
494 mAbs variants not monitored using CEX [119].

495 Jungbauer demonstrated in 1993 the combined effect of a linear salt- and pH-gradient  
496 in IEX mode for the separation of protein isoforms of a human monoclonal antibody [120]. The  
497 IEX chromatogram was compared with IEF, and confirmation of elution order based on pI was  
498 shown. As the method relied on the reaction of mannitol with borate, the broad-scale applicative  
499 value was limited. Many publications have investigated internally generated pH-gradient CEX  
500 methods to separate mAb charge variants, however, they often employ cationic buffering agents  
501 which can lead to interactions with the stationary-phase chemistry. This deviates the shape of  
502 the applied pH-gradient from the ideal linear case, affecting protein retention and the resolution  
503 of the separation [121-123]. In an attempt to address this issue, research groups have  
504 investigated algorithms to correct for these deviations [107], a simple mixture of buffering  
505 species which produce an internal linear gradient for neutral and acidic mAbs [124], mixed-bed  
506 stationary phases consisting of small-pore weak IEX and large-pore strong IEX particles  
507 allowing for independent internal pH-gradient generation and protein binding [125,126],

508 external pH gradients in anion-exchange mode using a mixture of amine buffering species as  
509 an application buffer and weakly acidic compounds as an elution buffer [127-129], shallow  
510 externally generated pH gradient of diethanolamine buffer on monolithic IEX stationary phases  
511 [130,131].

512 Another way of solving this issue is by using zwitterionic and acidic buffer substances  
513 with a pKa-range evenly distributed over the pH range and externally generate a pH and salt  
514 gradient. Typically, zwitterionic compounds tailored for biochemical research are used as  
515 buffering agents. It was shown that this allows for generating highly linear pH gradients, with  
516 even distribution of buffer capacity, for the analysis of charge heterogeneity of mAbs [132].  
517 Recently the ruggedness of a controlled gradient pH-formation with a zwitterionic buffer  
518 system for the separation of mAb charge variants was demonstrated, showing good robustness  
519 of the method with < 0.8% RSD for the retention times after more than 300 injections [133].

520

### 521 **3 Protein mass spectrometry**

522 Mass spectrometry (MS) for intact protein analysis has proven to be essential in the field  
523 of biomolecule characterization. Fenn received the Nobel Prize in Chemistry in 2002 for the  
524 development of electrospray ionization (ESI), allowing the transfer of biomacromolecules from  
525 an aqueous solution into the gas-phase as molecular ions without fragmentation [134,135]. ESI  
526 can operate in the flow regime from 1 mL/min. down to tens of nL/min., with the latter approach  
527 typically utilizing “static” (i.e., off-line) spray from glass capillaries, also called nano-ESI  
528 [136]. Electrospray is now the dominant ionization method in many chemical, (bio-)medical  
529 and pharmaceutical mass spectrometry laboratories, largely due to the ease with which it can  
530 be used to interface LC “in-line” with different types of MS(/MS) instruments [137].  
531 Denaturing MS-based strategies have been extensively applied to retrieve information on the

532 intact mass of therapeutic proteins, including information on the amino-acid sequence and post-  
533 translational modifications, the DAR and drug load distribution, etc [138].

534 A visualization of the different states of protein MS analysis is depicted in Fig. 5.  
535 Proteins encountered at physiological conditions remain their native 3D structure. In “intact  
536 denatured proteins” the 3D protein conformation is lost. The protein mass is particularly  
537 important when variations of the amino-acid sequence, such as mutations or truncations, as well  
538 as post-translational or chemical modifications, e.g., deamidation, covalent linkers, need to be  
539 identified and quantified [138]. While the full set of modifications present as well as  
540 heterogeneity arising from the occupancy of the possible sites can be obtained from intact,  
541 denaturing MS, mapping the modification sites requires MS/MS approaches typically using  
542 bottom-up proteomics, but increasingly also middle-down and top-down MS/MS [139]. The  
543 often overlooked, but important shortcoming of these “standard” proteomics methods however  
544 is that they usually only give partial sequence information (i.e. not all expected peptides or  
545 MS/MS fragments are found back in the spectra), and therefore neither identify all modification  
546 sites nor typically characterize the full complement of modifications, i.e., their extent and  
547 heterogeneity). It has become increasingly obvious that the full knowledge of the primary  
548 sequence information, the “proteoform”, i.e., the “chemical sum formula” of the protein and its  
549 sequence) [140], can only be obtained by a combination of intact protein MS with MS/MS  
550 approaches as they are used in proteomics, with or without prior digestion.

551 Extending the applicability of ESI-MS incorporating volatile buffer systems and  
552 physiological pH conditions, as well as modifications to the instruments to increase the mass  
553 range and the control over desolvation conditions, has led to the development of native MS  
554 [141,142]. Native MS has been extensively applied to study macromolecular assemblies,  
555 including stoichiometry and identity of binding partners [143,144], and in the last decade its  
556 applicability has been extended towards the MS analysis of biopharmaceutical products [145].



557 In native MS, it is believed that non-covalent weak interactions, i.e., van der Waals interactions,  
558 hydrogen bonds, electrostatic interactions, are maintained, preserving the higher-order, three-  
559 dimensional protein structure during the MS analysis. It is generally recognized that changes in  
560 charge density in ESI-MS spectra correspond to conformational changes, i.e., the tertiary  
561 protein structure [146]. Fig. 6A displays the charge-state distribution profile of an intact protein  
562 (anti-thrombin III) applying native MS conditions [147]. Due to the compact, folded state of  
563 the protein, the exposed surface that can be protonated is relatively small, therefore yielding a  
564 relatively narrow charge envelope situated in the high  $m/z$  region (low  $z$ ) compared to the same  
565 protein when applying denaturing ESI-MS conditions (Fig. 6C). Fig. 6B shows that native and  
566 denatured protein states coexist at equilibrium applying mildly denaturing conditions. The  
567 intermediate charge-density ions correspond to proteins that contain domains that are unfolded,  
568 while other domains retain their native conformation. While unfolding proteins in denaturing  
569 MS usually allows accurate and precise mass determination ( $\leq 1$  Da), desolvation conditions  
570 are more gentle in native MS and the folded protein often retains bound water or buffer ions,  
571 leading to a somewhat increased experimental mass compared to the expected value [148].  
572 When determining the intact mass of proteins above 100 kDa on the other hand, the native  
573 approach may become easier, as it produces fewer and lower charge states, whereas denaturing  
574 MS leads to a large number of closely spaced, highly charged peaks which are difficult to  
575 resolve and to correctly assign.

576 Ion mobility (IM) is now often coupled with native MS and several commercial  
577 platforms offer this option [142]. In ion mobility, ions are separated by their collision cross  
578 section (CCS), measured in  $\text{nm}^2$  or  $\text{\AA}^2$ , which depends on their charge but also their rotationally  
579 averaged size and shape – somewhat similar to gas-phase electrophoresis [149]. At each  $m/z$ ,  
580 different co-existing conformers, isomers or complex/aggregate topologies can be resolved as  
581 long as they differ in overall size by 2-3%. The measured mobilities of ions can be converted

582 to CCS values using a set of calibrants (e.g. protein standards) with known structure. This  
583 technology has come to the fore in the last 10 years and recent examples include studies of  
584 protein folding/misfolding and aggregation, intrinsic disorder phenomena and the identification  
585 of isomeric forms of metabolites, biomolecules and complexes [150]. In the context of  
586 biopharmaceuticals characterization, ion mobility has shown to be able to distinguish different  
587 glycoforms, even in cases where they cannot be resolved in LC, as well as disulfide isoforms  
588 [151].

589

### 590 **3.1 Conditions for direct infusion and hyphenation to LC**

591 Gentle ionization, in which the non-covalent interactions involved in protein higher-  
592 order structure, i.e., folding and interactions, are maintained, is considered to be a critical step  
593 in native MS [146]. Most native MS is done in “static”, off-line nano-electrospray ionization  
594 (nano-ESI) using metallized glass capillaries, also called direct infusion, with a flow rate < 20  
595 nL/min in order to minimize sample consumption, improve the tolerance of spraying aqueous  
596 buffer solutions, limiting the salt intake, and eliminating the need for desolvation gas and  
597 heating. Native MS can also be implemented at flow rates in the 200-300 nL/min. range which  
598 are compatible with in-line nano-LC, and in principle also at higher flow rates, although care  
599 has to be taken that ESI interface settings such as (hot) desolvation gas and source heating do  
600 not unfold the protein. Sample requirements for native MS and buffer conditions have been  
601 described by Hernandez and Robinson [152]. Typically, infusion of analyte at 1-20  $\mu$ M  
602 dissolved in 10 mM – 1 M aqueous ammonium acetate solution maintained near pH 7 or at the  
603 pH of choice, using an excess of ammonia or acetic acid, provides good MS spectra. Also, other  
604 ammonium salts and ammonium derivatives have been employed but acetates are found to  
605 perform better than bicarbonates [153]. Non-volatile ions such as sodium and potassium are  
606 minimized using buffer exchange and other desalting methods, since these salts induce adduct

607 formation, thereby lowering the mass resolution or suppressing signal entirely. Essential co-  
608 factors such as e.g. Mg or Zn ions can be added, but a large excess should be avoided. With  
609 respect to optimization of the MS settings, it is important that pressure in the transfer region  
610 between source and analyzer is optimized to ensure transmission of biomacromolecules.  
611 Modifications of MS instrumentation has been described in more detail by Rosati et al. [151].

612         Due to the stringent requirements with respect to infusion conditions, the number of  
613 reports describing the direct coupling between native LC and mass spectrometry is limited. First  
614 of all, the flow rate compatibility with LC constitutes a problem. Conventional SEC, HIC, and  
615 IEX separations are still performed using either 4.6 mm i.d. columns operated at a flow rate of  
616 1 mL/min, or 2.1 mm i.d. columns operated at 0.2 mL/min. Hence, post-column flow splitting  
617 is required to achieve direct coupling to MS via nano-ESI. Furthermore, the salts typically  
618 applied in SEC, HIC and IEX modes are incompatible with MS analysis. In case of aqueous  
619 SEC, the phosphate buffer can be replaced by an acetate buffer. In gel filtration, typical buffers  
620 are fully native, but scaling down is a major bottleneck. The sulfate ions typically used in HIC  
621 systems are also incompatible with MS, leading to significant signal suppression [154]. Volatile  
622 buffer acetate and tartrate and ammonium salt systems can be considered for HIC-MS analysis,  
623 but it should be noted that the choice affects protein retention and may limit the applicability.  
624 Xiu et al. reported a lack of retention for the HIC analysis of hydrophilic proteins using  
625 ammonium acetate as the mobile phase (as can be expected from the Hofmeister series) [154].  
626 Ammonium tartrate dissolved in an ammonium acetate buffer provided similar elution strength  
627 compared to ammonium sulfate. The MS compatibility with respect to adduct formation was  
628 only demonstrated after desalting using ultra-centrifugation followed by RP-LC-MS analysis.  
629 It has been reported by Chen et al. that the desalting processes can induce variations in the  
630 conformation of the proteins, and hence the native conformation may be lost [155]. A viable

631 approach to online HIC-ESI-MS was proposed by Chen et al., which involves the use of low  
632 concentrations of ammonium acetate mobile phases (volatile and MS compatible) [155].

633

### 634 **3.2 MS characterization of mAbs and ADCs: key examples**

635 A protocol for conducting native MS analysis of mAbs and ADCs has been described  
636 by Thompson et al. [146]. Illustrative MS spectra of a 145 kDa purified mAb via direct infusion  
637 are demonstrated in Fig. 7A, yielding only seven charge states. A mass accuracy of 5 Da allows  
638 establishing the protein i.d. with high confidence when the amino-acid sequence is known and  
639 allows identifying modifications, including primary sequence mutations and C-terminal lysine  
640 clipping [146]. The natural isotopic peak width of the intact antibody was estimated to be 25  
641 Da. ~~A very accurate isotope pattern needs to be recorded in order. Hence, the mass resolution~~  
642 ~~currently achieved using time-of-flight instruments is too low~~ to detect modifications such as  
643 deamidation, yielding a mass increase of +1 Da. Significant improvements in resolution and  
644 native MS technology have been reported over the years. For example, in 2012, Rose et al.  
645 reported the use of Orbitrap MS yielding a resolution of 16,000 at m/z 10,000 [156]. The  
646 applicability of native MS to probe the binding stoichiometries and affinities of mAb-antigen  
647 complexes was first demonstrated by Tito et al. [ref157]. Compared to SEC/UV or SPR  
648 spectroscopy yielding evidence for binding, or at best average-weight information, native MS  
649 provides accurate mass information. Tito et al. also performed control experiments to establish  
650 the specificity of the interactions [157].

651 The presence of microheterogeneities in the protein chains can derive from  
652 inconsistencies in the production process (differences in the cell lines) and therefore it is  
653 extremely important to perform batch to batch quality control of the mAbs before their  
654 application as therapeutics. Most of the times these inconsistencies stem from heterogeneous  
655 glycosylation patterns. Fig. 7B shows native MS spectra of a mAb with glycosylation and after

656 deglycosylation using peptide-N-glycosidase F [146]. The presence of glycans increases both  
657 the mass and the heterogeneity of the MS signal, that in turns decreases the peak intensity. Intact  
658 MS analysis can be used to reveal the presence of different glycoforms or on the chains of the  
659 mAbs (mutations on the mAbs chain can dramatically alter the glycosylation) [ref]. Rosati et  
660 al. performed both qualitative and quantitative analysis of glycosylation profiles on mAbs using  
661 high-resolution Orbitrap MS technology [151]. Fig. 8 compares native MS spectra of IgGs  
662 obtained via direct-infusion experiment and ~~that obtained~~ after on-line SEC analysis, as  
663 performed by Chatterjee and Sobott. This experiment showed that the SEC analysis induced  
664 partially unfolding of the antibodies (without breaking disulfide bonds), as it appears with higher  
665 charge states.

666 With respect to the analysis of ADCs, MS enables the characterization of the drug load  
667 profile and distribution, and the DAR. Valliere-Douglas et al. and Sobott et al. reported on a  
668 method allowing to determine the intact mass of an ADC composed of non-covalently-  
669 associated heavy and light chains, with a drug linked to interchain cysteine residues [158, 159].  
670 Debaene et al. conducted native MS experiments of Brentuximab vedotin (also an inter-chain  
671 cysteinyl-linked ADC) providing accurate mass measurements of intact ADCs together with  
672 the average DAR and drug distribution [160]. The same group also characterized a lysine linked  
673 antibody drug conjugate (Tratuzumab emtansine) [160]. Extending the glycoprofiling  
674 experiments of mAbs, Rosati et al. also characterized the drug load and glycosylation patterns  
675 on an IgG4 ADCs using high-resolution native MS [151].

676

#### 677 **4 Concluding remarks**

678 Advances in the development of biotherapeutics are closely followed by innovations in  
679 the field of separation sciences and mass spectrometry. The chemical heterogeneity of  
680 biopharmaceuticals in terms of polarity, size, and charge, require the use of complementary

681 native LC techniques ideally hyphenated to mass spectrometry to fully characterize (and  
682 quantify) the complex protein samples. This requires the use of separation technology with high  
683 resolving power to achieve the highest confidence in elucidating the biopharmaceutical product.  
684 Although columns packed with sub-2- $\mu\text{m}$  particles are being introduced and have become  
685 commercially available, the majority of LC experiments is still performed using conventional  
686 columns packed with 5  $\mu\text{m}$  particles. However, to make a successful transition the effects on  
687 protein unfolding induced by the mobile-phase composition applied, shear stress, and thermal  
688 effects, need to be critically assessed. Furthermore, the pressure stability of currently available  
689 IEX, SEC, and HIC columns needs to be augmented in order to allow for operating pressures  
690 above 50 MPa. A promising (but currently underestimated) stationary-phase type for  
691 biomacromolecule separation may be monolithic columns. The morphology can be optimized  
692 to achieve high efficiency separations by down-scaling the globule size, while the macropore  
693 size can be tuned to minimize shear stress.

694 Conventional 4.6 mm i.d. analytical columns for mAb analysis, require several  
695 micrograms of mAbs to achieve adequate detection sensitivity of low-abundant sample species.  
696 The yield of biopharmaceutical products coming from microwell-plate cell cultures is however  
697 limited and often insufficient for high-resolution LC analysis. This mandates the  
698 miniaturization of column formats allowing to increase detection sensitivity and to diminish  
699 sample consumption. It should be noted however, that extra-column band broadening needs to  
700 be minimized, imposing stringent requirements on instrumentation. An additional advantage of  
701 reducing the column format, is that it decreases the salt-intake at the MS interface, effectively  
702 improving MS compatibility. The use of organic solvents that are conventionally added to the  
703 mobile-phase, not only to improve spray drying but also to reduce the surface tension of the  
704 spray droplets leading to higher ionization yields, should be limited when performing  
705 bioanalysis. This is not only mandatory to maintain the protein conformation but also because

706 buffers are known to lead to suppression of ion formation in the ion source and ion source  
707 contamination due to salt crust formation. Novel salt systems, buffering agents, the effects of  
708 ionic strength have to be further studied in order to improve MS compatibility. At the same  
709 time, it is mandatory to further study the effects of ionization conditions and MS conditions on  
710 protein conformation, in order to establish relevant biological conditions.

711

712 **List of abbreviations**

713 ADC Antibody drug conjugate

714 CCS Collision cross section

715 CDRs Complementarity determining regions

716 CHO Chines Hamster Ovary

717 DAR Drug to antibody ratio

718 E. Coli Escherichia Coli

719 HIC Hydrophobic interaction chromatography

720 IgG Immunoglobulin G

721 mAb Monoclonal antibody

722 PTM Post translational modification

723

724 **65 Acknowledgments**

725 JDV acknowledges a post-doctoral research grant of the Research Foundation Flanders  
726 (FWO – grant no. 12J6517N) and SC acknowledges a PhD research grant from the Institute for  
727 Innovation through Science and Technology (IWT). Dr. Koen Sandra (RIC, Kortrijk, Belgium)  
728 is acknowledged for providing Figure 1. Jonas-Frederik Jans (VUB) is acknowledged for his  
729 assistance in the preparation of the review manuscript.

730

731 **67 References**

732 [1] <http://www.persistencemarketresearch.com/mediarelease/biopharmaceutical-market.asp>  
733 (last time accessed: May 12, 2017).



- 734 [2] <http://www.mckinsey.com/industries/pharmaceuticals-and-medical-products/our->  
735 [insights/rapid-growth-in-biopharma](http://www.mckinsey.com/industries/pharmaceuticals-and-medical-products/our-insights/rapid-growth-in-biopharma) (last time accessed: July 7, 2017).
- 736 [3] Walsh, G., Biopharmaceutical benchmarks 2014. *Nat. Biotechnol.* 2014, 32, 992–1000.
- 737 [4] Leader, B., Baca, Q. J., Golan, D. E., Protein therapeutics: a summary and pharmacological  
738 classification. *Nat. Rev. Drug Discov.* 2008, 7, 21–39.
- 739 [5] Bray, G. L., Gomperts, E. D., Courter, S., Gruppo, R., Gordon, E. M., Manco-Johnson, M.,  
740 Shapiro, A., Scheibel, E., White, G. 3<sup>rd</sup>, Lee, M. A., multicenter study of recombinant factor  
741 VIII (recombinate): safety, efficacy, and inhibitor risk in previously untreated patients with  
742 hemophilia A. The Recombinate Study Group. *Blood*, 1994, 83, 2428–2435.
- 743 [6] Weiner, L. M., Surana, R., Wang, S., Monoclonal antibodies: versatile platforms for cancer  
744 immunotherapy. *Nat. Rev. Immunol.* 2010, 10, 317–327.
- 745 [7] Weiner, L. M., Surana, R., Wang, S., Monoclonal antibodies: versatile platforms for cancer  
746 immunotherapy. *Nat. Rev. Immunol.* 2010, 10, 317–327.
- 747 [8] Rostami, A. S., Qazi A.I., Sikorski, A.R. The clinical landscape of antibody drug  
748 conjugated. ADC review. <https://adcreview.com/articles/doi-10-14229jadc-2014-8-1-001/>
- 749 [9] Ohtake, S., Arakawa, T., Recombinant therapeutic protein vaccines. *Protein Pept. Lett.*  
750 2013, 20, 1324–1344.
- 751 [10] Ecker, D. M., Jones, S. D., Levine, H. L., The therapeutic monoclonal antibody market.  
752 *mAbs* 2015, 20, 9–14.
- 753 [11] Mack, F., Ritchie, M., Sapra, P., The next generation of antibody drug conjugates. *Semin.*  
754 *Oncol.* 2014, 41, 637–652.
- 755 [12] Helliwell, C. L., Coles, A. J., Monoclonal antibodies in multiple sclerosis treatment:  
756 current and future steps. *Ther. Adv. Neurol. Disord.* 2009, 2, 195–203.

- 757 [13] Tanaka, T., Hishitani, Y., Ogata, A., Monoclonal antibodies in rheumatoid arthritis:  
758 comparative effectiveness of tocilizumab with tumor necrosis factor inhibitors. *Biol. Targets*  
759 *Ther.* 2014, 8, 141–153.
- 760 [14] Li, F., Vijayasankaran, N., Shen, A. Y., Kiss, R., Amanullah, A., Cell culture processes  
761 for monoclonal antibody production. *mAbs* 2010, 2, 466–477.
- 762 [15] Milstein, C., The hybridoma revolution: an offshoot of basic research. *BioEssays* 1999, 21,  
763 966–973.
- 764 [16] Carvalho, L. S., Silva, O. B. da, deAlmeida, G. C., Oliveira, J. D. de, Carmo, N. S. P. and  
765 T. S., Production processes for monoclonal antibodies. 2017, DOI: 10.5772/64263.
- 766 [17] Nelson, A. L., Antibody fragments. *mAbs* 2010, 2, 77–83.
- 767 [18] Nimmerjahn, F., Ravetch, J. V., Fcγ receptors as regulators of immune responses.  
768 *Nat. Rev. Immunol.* 2008, 8, 34–47.
- 769 [19] Kontermann, R., Dual targeting strategies with bispecific antibodies. *mAbs*, 2012, 4, 182–  
770 197.
- 771 [20] Kontermann, R. E., Brinkmann, U., Bispecific antibodies. *Drug Discov. Today*, 2015, 15,  
772 838–847.
- 773 [21] Diamantis, N., Banerji, U., Antibody-drug conjugates-an emerging class of cancer  
774 treatment. *Br. J. Cancer* 2016, 114, 362–367.
- 775 [22] Van de Donk, N. W. C. J., Dhimolea, E., Brentuximab vedotin. *mAbs* 2012, 4, 458–465.
- 776 [23] Lambert, J. M., Chari, R. V. J., Ado-trastuzumab Emtansine (T-DM1): an antibody-drug  
777 conjugate (ADC) for HER2-positive breast cancer. *J. Med. Chem.* 2014, 57, 6949–6964.
- 778 [24] Fan, G., Wang, Z., Hao, M., Li, J., Bispecific antibodies and their applications. *J. Hematol.*  
779 *Oncol.* 2015, 8, 130.

780 [25] Berkowitz, S. A., Engen, J. R., Mazzeo, J. R., Jones, G. B., Analytical tools for  
781 characterizing biopharmaceuticals and the implications for biosimilars. *Nat. Rev. Drug Discov.*  
782 2012, 11, 527–540.

783 [26] Bosques, C. J., Collins, B. E., Meador, J. W., Sarvaiya, H., Murphy, J. L., Dellorusso, G.,  
784 Bulik, D. A., Hsu, I.-H., Washburn, N., Sipsy, S. F., Myette, J. R., Raman, R., Shriver, Z.,  
785 Sasisekharan, R., Venkataraman, G., Chinese hamster ovary cells can produce galactose- $\alpha$ -1,3-  
786 galactose antigens on proteins. *Nat. Biotechnol.* 2010, 28, 1153–1156.

787 [27] Narhi, L. O., Jiang, Y., Cao, S., Benedek, K., Shnek, D., A critical review of analytical  
788 methods for subvisible and visible particles. *Curr. Pharm. Biotechnol.* 2009, 10, 373–381.

789 [28] Parr, M. K., Montacir, O., Montacir, H., Physicochemical characterization of  
790 biopharmaceuticals. *J. Pharm. Biomed. Anal.* 2016, 130, 366–389.

791 [29] Bush, D. R., Zang, L., Belov, A. M., Ivanov, A. R., Karger, B. L., High Resolution CZE-  
792 MS Quantitative Characterization of Intact Biopharmaceutical Proteins: Proteoforms of  
793 Interferon- $\beta$ 1. *Anal. Chem.* 2016, 88, 1138–1146.

794 [30] Hayes, J. M., Frostell, A., Karlsson, R., Müller, S., Millan-Martin, S., Pauers, M., Reuss,  
795 F., Cosgrave, E., Anneren, C., Davey, G. P., Rudd, P. M., Identification of Fc gamma receptor  
796 glycoforms that produce differential binding kinetics for rituximab. *Mol. Cell. Proteomics MCP*  
797 2017, in press.

798 [31] Lindqvist, B., Storgards, T., Molecular-sieving properties of starch. *Nature* 1955, 175,  
799 511–512.

800 [32] De Vos, J., Kaal, E. R., Swart, R., Baca, M., Heyden, Y. Vander, Eeltink, S., Aqueous  
801 size-exclusion chromatographic separations of intact proteins under native conditions: Effect  
802 of pressure on selectivity and efficiency. *J. Sep. Sci.* 2016, 39, 689–695.

803 [33] Goyon, A., Beck, A., Colas, O., Sandra, K., Guillarme, D., Fekete, S., Evaluation of size  
804 exclusion chromatography columns packed with sub-3  $\mu\text{m}$  particles for the analysis of  
805 biopharmaceutical proteins. *J. Chromatogr. A* 2017, 1498, 80–89.

806 [34] Goyon, A., Guillarme, D., Fekete, S., The importance of system band broadening in  
807 modern size exclusion chromatography. *J. Pharm. Biomed. Anal.* 2017, 135, 50–60.

808 [35] Fekete, S., Ganzler, K., Guillarme, D., Critical evaluation of fast size exclusion  
809 chromatographic separations of protein aggregates, applying sub-2  $\mu\text{m}$  particles. *J. Pharm.*  
810 *Biomed. Anal.* 2013, 78-79, 141–149.

811 [36] Diederich, P., Hansen, S. K., Oelmeier, S. A., Stolzenberger, B., Hubbuch, J., A sub-two  
812 minutes method for monoclonal antibody-aggregate quantification using parallel interlaced size  
813 exclusion high performance liquid chromatography. *J. Chromatogr. A* 2011, 1218, 9010–9018.

814 [37] Farnan, D., Moreno, G. T., Stults, J., Becker, A., Tremintin, G., van Gils, M., Interlaced  
815 size exclusion liquid chromatography of monoclonal antibodies. *J. Chromatogr. A* 2009, 1216,  
816 8904–8909.

817 [38] Bouvier, E. S. P., Koza, S. M., Advances in size-exclusion separations of proteins and  
818 polymers by UHPLC. *TrAC Trends Anal. Chem.* 2014, 63, 85–94.

819 [39] Wyndham, K. D., O’Gara, J. E., Walter, T. H., Glose, K. H., Lawrence, N. L., Alden, B.  
820 A., Izzo, G. S., Hudalla, C. J., Iraneta, P. C., Characterization and evaluation of C18 HPLC  
821 stationary phases based on ethyl-bridged hybrid organic/inorganic particles. *Anal. Chem.* 2003,  
822 75, 6781–6788.

823 [40] Kopaciewicz, W., Regnier, F. E., Nonideal size-exclusion chromatography of proteins:  
824 Effects of pH at low ionic strength. *Anal. Biochem.* 1982, 126, 8–16.

825 [41] Ricker, R. D., Sandoval, L. A., Fast, reproducible size-exclusion chromatography of  
826 biological macromolecules. *J. Chromatogr. A* 1996, 743, 43–50.

827 [42] Goyon, A., Beck, A., Veuthey, J.-L., Guillaume, D., Fekete, S., Comprehensive study on  
828 the effects of sodium and potassium additives in size exclusion chromatographic separations of  
829 protein biopharmaceuticals. *J. Pharm. Biomed. Anal.* 2017, 144, 242–251.

830 [43] Gervais, D., Downer, A., King, D., Kanda, P., Foote, N., Smith, S., Robust quantitation of  
831 basic-protein higher-order aggregates using size-exclusion chromatography. *J. Pharm. Biomed.*  
832 *Anal.* 2017, 139, 215–220.

833 [44] Zheng, J. Y., Janis, L. J., Influence of pH, buffer species, and storage temperature on  
834 physicochemical stability of a humanized monoclonal antibody LA298. *Int. J. Pharm.* 2006,  
835 308, 46–51.

836 [45] Dada, O. O., Rao, R., Jones, N., Jaya, N., Salas-Solano, O., Comparison of SEC and CE-  
837 SDS methods for monitoring hinge fragmentation in IgG1 monoclonal antibodies. *J. Pharm.*  
838 *Biomed. Anal.* 2017, 145, 91–97.

839 [46] Liu, H., Gaza-Bulsecu, G., Chumsae, C., Analysis of reduced monoclonal antibodies using  
840 size exclusion chromatography coupled with mass spectrometry. *J. Am. Soc. Mass Spectrom.*  
841 2009, 20, 2258–2264.

842 [47] Boysen, M., Schlicksupp, L., Dreher, I., Loebbert, R., Richter, M., SEC based method for  
843 size determination of immune complexes of therapeutic antibodies in animal matrix. *J.*  
844 *Immunol. Res.* 2016 (Article ID 9096059) 1–9.

845 [48] Kükler, B., Filipe, V., van Duijn, E., Kasper, P. T., Vreeken, R. J., Heck, A. J. R., Jiskoot,  
846 W., Mass spectrometric analysis of intact human monoclonal antibody aggregates fractionated  
847 by size-exclusion chromatography. *Pharm. Res.* 2010, 27, 2197–2204.

848 [49] Shen, M. L., Benson, L. M., Johnson, K. L., Lipsky, J. J., Naylor, S., Effect of enzyme  
849 inhibitors on protein quaternary structure determined by on-line size exclusion

850 chromatography-microelectrospray ionization mass spectrometry. *J. Am. Soc. Mass Spectrom.*  
851 2001, 12, 97–104.

852 [50] Valliere-Douglass, J. F., McFee, W. A., Salas-solano, O., Native intact mass determination  
853 of antibodies conjugated with monomethyl auristatin E and F at interchain Cysteine Residues.  
854 *Anal. Chem.* 2012, 84, 2843–2849.

855 [51] Lazar, A. C., Wang, L., Blättler, W. A., Amphlett, G., Lambert, J. M., Zhang, W., Analysis  
856 of the composition of immunoconjugates using size-exclusion chromatography coupled to mass  
857 spectrometry. *Rapid Commun. Mass Spectrom.* 2005, 19, 1806–1814.

858 [52] Brady, L. J., Valliere-Douglass, J., Martinez, T., Balland, A., Molecular mass analysis of  
859 antibodies by on-line SEC-MS. *J. Am. Soc. Mass Spectrom.* 2008, 19, 502–509.

860 [53] Wakankar, A., Chen, Y., Gokarn, Y., Jacobson, F. S., Analytical methods for  
861 physicochemical characterization of antibody drug conjugates. *MAbs.* 2011, 3, 161–172.

862 [54] Bobály, B., Fleury-Souverain, S., Beck, A., Veuthey, J.-L., Guillarme, D., Fekete, S.,  
863 Current possibilities of liquid chromatography for the characterization of antibody-drug  
864 conjugates. *J. Pharm. Biomed. Anal.* 2017, in press.

865 [55] Rea, J. C., Moreno, G. T., Vampola, L., Lou, Y., van Haan, B., Tremintin, G., Simmons,  
866 L., Nava, A., Wang, Y. J., Farnan, D., Capillary size exclusion chromatography with picogram  
867 sensitivity for analysis of monoclonal antibodies purified from harvested cell culture fluid. *J.*  
868 *Chromatogr. A* 2012, 1219, 140–146.

869 [56] Smoluch, M. T., Mak, P., Chervet, J. P., Höhne, G., Silberring, J., Size-exclusion  
870 chromatography performed in capillaries. Studies by liquid chromatography-mass  
871 spectrometry. *J. Chromatogr. B Biomed. Sci. Appl.* 1999, 726, 37–43.

872 [57] Fekete, S., Beck, A., Veuthey, J.-L., Guillarme, D., Theory and practice of size exclusion  
873 chromatography for the analysis of protein aggregates. *J. Pharm. Biomed. Anal.* 2014, 101,  
874 161–173.

875 [58] Farrell, A., Jakes, C., Ley, A., De Pra, M., Steiner, F., Bones, J. Lifetime stability of size  
876 exclusion chromatography columns for protein aggregate analysis. Thermo Fisher Scientific,  
877 application note 2017, 72362, 1–6.

878 [59] De Vos, J., Stassen, C., Vaast, A., Desmet, G., Eeltink, S., High-resolution separations of  
879 tryptic digest mixtures using core-shell particulate columns operated at 1200 bar. *J.*  
880 *Chromatogr. A* 2012, 1264, 57–62.

881 [60] Tanaka, N., McCalley, D. V., Core-shell, ultra small particles, monoliths, and other support  
882 materials in high-performance liquid chromatography. *Anal. Chem.* 2016, 88, 279–298.

883 [61] Pirok, B. W. J., Breuer, P., Hoppe, S. J. M., Chitty, M., Welch, E., Farkas, T., van der Wal,  
884 S., Peters, R., Schoenmakers, P. J., Size-exclusion chromatography using core-shell particles.  
885 *J. Chromatogr. A* 2017, 1486, 96–102.

886 [62] De Vos, J., Broeckhoven, K., Eeltink, S., Advances in ultrahigh-pressure liquid  
887 chromatography technology and system design. *Anal. Chem.* 2016, 88, 262–278.

888 [63] Striegel, A. M., Observations regarding on-column, flow-induced degradation during SEC  
889 analysis. *J. Liq. Chromatogr. Relat. Technol.* 2008, 31,3105–3114.

890 [64] Tiselius, A., Adsorption separation by salting out. *Arkiv for Mimi, Mineral. Geol.* (1948)  
891 26B, 1–5.

892 [65] Queiroz, J. A., Tomaz, C. T., Cabral, J. M. S., Hydrophobic interaction chromatography  
893 of proteins. *J. Biotechnol.* 2001, 87, 143–159.

894 [66] Pace, C. N., Fu, H., Fryar, K. L., Landua, J., Trevino, S. R., Shirley, B. A., Hendricks, M.  
895 M., Iimura, S., Gajiwala, K., Scholtz, J. M., Grimsley, G. R., Contribution of hydrophobic  
896 Interactions to protein stability. *J. Mol. Biol.* 2011, 408, 514–528.

897 [67] Lienqueo, M. E., Mahn, A., Salgado, J. C., Asenjo, J. A., Current insights on protein  
898 behaviour in hydrophobic interaction chromatography. *J. Chromatogr. B* 2007, 849, 53–68.

899 [68] Szepesy, L., Rippel, G., Comparison and evaluation of HIC columns of different  
900 hydrophobicity. *Chromatographia* 1992, 34, 391–397.

901 [69] Fekete, S., Veuthey, J.-L., Beck, A., Guillarme, D., Hydrophobic interaction  
902 chromatography for the characterization of monoclonal antibodies and related products. *J.*  
903 *Pharm. Biomed. Anal.* 2016, 130, 3–18.

904 [70] Baca, M., De Vos, J., Bruylants, G., Bartik, K., Liu, X., Cook, K., Eeltink, S., A  
905 comprehensive study to protein retention in hydrophobic interaction chromatography. *J.*  
906 *Chromatogr. B* 2016, 1032, 182–188.

907 [71] Mahn, A., Lienqueo, M. E., Asenjo, J. A., Optimal operation conditions for protein  
908 separation in hydrophobic interaction chromatography. *J. Chromatogr. B* 2007, 849, 236–242.

909 [72] Shimizu, S., McLaren, W. M., Matubayasi, N., The Hofmeister series and protein-salt  
910 interactions. *J. Chem. Phys.* 2006, 124, 234905.

911 [73] Baldwin, R. L., How Hofmeister ion interactions affect protein stability. *Biophys. J.* 1996,  
912 71, 2056–2063.

913 [74] Arakawa, T., Timasheff, S. N., Preferential interactions of proteins with salts in  
914 concentrated solutions. *Biochemistry* 1982, 21, 6545–6552.

915 [75] Rodriguez-Aller, M., Guillarme, D., Beck, A., Fekete, S., Practical method development  
916 for the separation of monoclonal antibodies and antibody-drug-conjugate species in



917 hydrophobic interaction chromatography, part 1: optimization of the mobile phase. *J. Pharm.*  
918 *Biomed. Anal.* 2016, 118, 393–403.

919 [76] Fausnaugh, J. L., Kennedy, L. A., Regnier, F. E., Comparison of hydrophobic-interaction  
920 and reversed-phase chromatography of proteins. *J. Chromatogr.* 1984, 317, 141–155.

921 [77] Haidacher, D., Vailaya, A., Horváth, C., Temperature effects in hydrophobic interaction  
922 chromatography. *Proc. Natl. Acad. Sci.* 1996, 93, 2290–2295.

923 [78] Muca, R., Piątkowski, W., Antos, D., Altering efficiency of hydrophobic interaction  
924 chromatography by combined salt and temperature effects. *J. Chromatogr. A* 2009, 1216, 8712–  
925 8721.

926 [79] Bobaly, B., Beck, A., Veuthey, J.-L., Guillarme, D., Fekete, S., Impact of organic modifier  
927 and temperature on protein denaturation in hydrophobic interaction chromatography. *J. Pharm.*  
928 *Biomed. Anal.* 2016, 131, 124–132.

929 [80] Boyd, D., Kaschak, T., Yan, B., HIC resolution of an IgG1 with an oxidized Trp in a  
930 complementarity determining region. *J. Chromatogr. B* 2011, 879, 955–960.

931 [81] Valliere-Douglass, J., Wallace, A., Balland, A., Separation of populations of antibody  
932 variants by fine tuning of hydrophobic-interaction chromatography operating conditions. *J.*  
933 *Chromatogr. A* 2008, 1214, 81–89

934 [82] Le, L. N., Moore, J. M. R., Ouyang, J., Chen, X., Nguyen, M. D. H., Galush, W. J.,  
935 Profiling Antibody Drug Conjugate Positional Isomers: A System-of-Equations Approach.  
936 *Anal. Chem.* 2012, 84, 7479–7486.

937 [83] Cusumano, A., Guillarme, D., Beck, A., Fekete, S., Practical method development for the  
938 separation of monoclonal antibodies and antibody-drug-conjugate species in hydrophobic  
939 interaction chromatography, part 2: Optimization of the phase system. *J. Pharm. Biomed. Anal.*  
940 2016, 121, 161–173.

941 [84] Michels, D. A., Brady, L. J., Guo, A., Balland, A., Fluorescent derivatization method of  
942 proteins for characterization by capillary electrophoresis-sodium dodecyl sulfate with laser-  
943 induced fluorescence detection. *Anal. Chem.* 2007, 79, 5963–5971.

944 [85] Bobály, B., Fleury-Souverain, S., Beck, A., Veuthey, J.-L., Guillarme, D., Fekete, S.,  
945 Current possibilities of liquid chromatography for the characterization of antibody-drug  
946 conjugates. *J. Pharm. Biomed. Anal.* 2017, in press.

947 [86] Cohn, W. E., The separation of purine and pyrimidine bases and of nucleotides by ion  
948 exchange. *Science* 1949, 109, 377–378.

949 [87] Struble, E. B., Kirschbaum, N., Liu, J., Marszal, E., Shapiro, M., in: Sauna, Z. E., Kimchi-  
950 Sarfaty, C. (Eds.), *Protein Therapeutics*. Springer International Publishing, Cham 2016, pp. 69–  
951 122.

952 [88] Khawli, L. A., Goswami, S., Hutchinson, R., Kwong, Z. W., Yang, J., Wang, X., Yao, Z.,  
953 Sreedhara, A., Cano, T., Tesar, D., Nijem, I., Allison, D. E., Wong, P. Y., Kao, Y. H., Quan,  
954 C., Joshi, A., Harris, R. J., Motchnik, P., Charge variants in IgG1: Isolation, characterization,  
955 in vitro binding properties and pharmacokinetics in rats. *MABs* 2010, 2, 613–624.

956 [89] Rea, J. C., Freistadt, B. S., McDonald, D., Farnan, D., Wang, Y. J., Capillary ion-exchange  
957 chromatography with nanogram sensitivity for the analysis of monoclonal antibodies. *J.*  
958 *Chromatogr. A* 2015, 1424, 77–85.

959 [90] Harris, R. J., Kabakoff, B., Macchi, F. D., Shen, F. J., Kwong, M., Andya, J. D., Shire, S.  
960 J., Bjork, N., Totpal, K., Chen, A. B., Identification of multiple sources of charge heterogeneity  
961 in a recombinant antibody. *J. Chromatogr. B Biomed. Sci. Appl.* 2001, 752, 233–245.

962 [91] Fekete, S., Beck, A., Veuthey, J. L., Guillarme, D., Ion-exchange chromatography for the  
963 characterization of biopharmaceuticals. *J. Pharm. Biomed. Anal.* 2015, 113, 43–55.

- 964 [92] Weitzhandler, M., Farnan, D., Horvath, J., Rohrer, J. S., Slingsby, R. W., Avdalovic, N.,  
965 Pohl, C., Protein variant separations by cation-exchange chromatography on tentacle-type  
966 polymeric stationary phases, *J. Chromatogr. A* 1998, 828, 365–372.
- 967 [93] Roos, H. P., in: Kastner, M. (Eds.), *Protein Liquid Chromatography*. Elsevier, Amsterdam  
968 2000, pp. 3–88.
- 969 [94] Hodder, A. N., Aguilar, M. I., Hearn, M. T. N., High-performance liquid chromatography  
970 of amino acids, peptides and proteins XCVIII. The influence of different displacer salts on the  
971 bandwidth properties of proteins separated by gradient elution anion-exchange  
972 chromatography. *J. Chromatogr. A* 1990, 512, 41–56.
- 973 [95] Gooding, K. M., Schmuck, M. N., Ion selectivity in the high-performance cation-exchange  
974 chromatography of proteins. *J. Chromatogr. A* 1984, 296, 321–328.
- 975 [96] Kopaciewicz, W., Regnier, F. E., Mobile phase selection for the high-performance ion-  
976 exchange chromatography of proteins. *Anal. Biochem.* 1983, 133, 251–259.
- 977 [97] Singh, S. K., Narula, G., Rathore, A. S., Should charge variants of monoclonal antibody  
978 therapeutics be considered critical quality attributes? *Electrophoresis* 2016, 37, 2338–2346.
- 979 [98] Oorhouse, K. G., Nashabeh, W., Deveney, J., Bjork, N. S., Mulkerrin, M. G., Ryskamp,  
980 T., Validation of an HPLC method for the analysis of the charge heterogeneity of the  
981 recombinant monoclonal antibody IDEC-C2B8 after papain digestion. *J. Pharm. Biomed. Anal.*  
982 1997, 16, 593–603.
- 983 [99] Sluyterman, L. A. AE., Elgersma, O., Chromatofocusing: isoelectric focusing on ion-  
984 exchange columns: I. general principles. *J. Chromatogr. A* 1978, 150, 17–30.
- 985 [100] Sluyterman, L. A. AE., Wijdenes, J., Chromatofocusing: isoelectric focusing on ion-  
986 exchange columns: II. Experimental-verification. *J. Chromatogr. A* 1978, 150, 31–44.

987 [101] Sluyterman, L. A. AE., Wijdenes, J., Chromatofocusing: III. The properties of a deae-  
988 agarose anion exchanger and its suitability for protein separations. *J. Chromatogr. A* 1981, 206,  
989 429–440.

990 [102] Hearn, M. T. W., Lyttle, D. J., Buffer-focusing chromatography using multicomponent  
991 electrolyte elution systems. *J. Chromatogr. A* 1981, 218, 483–495.

992 [103] Pabst, T. M., Carta, G., Ramasubramanian, N., Hunter, A. K., Mensah, P., Gustafson, M.  
993 E., Separation of protein charge variants with induced pH gradients using anion-exchange  
994 chromatographic columns. *Biotechnol. Prog.* 2008, 24, 1096–1106.

995 [104] Pabst, T. M., Antos, D., Carta, G., Ramasubramanian, N., Hunter, A. K., Protein  
996 separations with induced pH gradients using cation-exchange chromatographic columns  
997 containing weak acid groups. *J. Chromatogr. A* 2008, 1181, 83–94.

998 [105] Scott, J. H., Kelner, K. L., Pollard, H. B., Purification of synexin by pH step elution from  
999 chromatofocusing media in the absence of ampholytes. *Anal. Biochem.* 1985, 149, 163–165.

1000 [106] Kröner, F., Hubbuch, J., Systematic generation of buffer systems for pH gradient ion  
1001 exchange chromatography and their application. *J. Chromatogr. A* 2013, 1285, 78–87.

1002 [107] Tsonev, L. I., Hirsh, A. G., Theory and applications of a novel ion exchange  
1003 chromatographic technology using controlled pH gradients for separating proteins on anionic  
1004 and cationic stationary phases. *J. Chromatogr. A* 2008, 1200, 166–182.

1005 [108] Tsonev, L. I., Hirsh, A., Improved resolution in the separation of monoclonal antibody  
1006 isoforms using controlled pH gradients in IEX chromatography. *Am. Biotechnol. Lab.* 2009, 27,  
1007 10–12.

1008 [109] He, Y., Isele, C., Hou, W., Ruesch, M., Rapid analysis of charge variants of monoclonal  
1009 antibodies with capillary zone electrophoresis in dynamically coated fused-silica capillary. *J.*  
1010 *Sep. Sci.* 2011, 34, 548–555.

1011 [110] Liu, H., Gaza-bulseco, G., Faldu, D., Chumsae, C., Sun, J., Heterogeneity of monoclonal  
1012 antibodies. *J. Pharm. Sci.* 2008, 97, 2426–2447.

1013 [111] Vlasak, J., Ionescu, R., Fragmentation of monoclonal antibodies. *MAbs* 2011, 3, 253–  
1014 263.

1015 [112] Chen, T., Chen, Y., Stella, C., Medley, C. D., Gruenhagen, J. A., Zhang, K., Antibody-  
1016 drug conjugate characterization by chromatographic and electrophoretic techniques. *J.*  
1017 *Chromatogr. B.* 2016, 1032, 39–50.

1018 [113] Ståhlberg, J., Retention models for ions in chromatography. *J. Chromatogr. A* 1999, 855,  
1019 3–55.

1020 [114] Stout, R. W., Sivakoff, S. I., Ricker, R. D., Snyder, L. R., Separation of proteins by  
1021 gradient elution from ion-exchange columns: optimizing experimental conditions. *J.*  
1022 *Chromatogr. A* 1986, 353, 439–463.

1023 [115] Schmidt, M., Hafner, M., Frech, C., Modeling of salt and pH gradient elution in ion-  
1024 exchange chromatography. *J. Sep. Sci.* 2014, 37, 5–13.

1025 [116] Fekete, S., Beck, A., Guillarme, D., Fekete, J., Method development for the separation of  
1026 monoclonal antibody charge variants in cation exchange chromatography, Part I: Salt gradient  
1027 approach. *J. Pharm Biomed. Anal.* 2015, 102, 33–44.

1028 [117] Fekete, S., Beck, A., Fekete, J., Guillarme D., Method development for the separation of  
1029 monoclonal antibody charge variants in cation exchange chromatography, Part II: pH gradient  
1030 approach. *J. Pharm. Biomed. Anal.* 2015, 102, 282–289.

1031 [118] Evans, W., Removing aggregates in monoclonal antibody purification. *Pharmaceutical*  
1032 *Technology* 2015, 39, 72–74.

1033 [119] Teshima, G., Li, M. X., Danishmand, R., Obi, C., To, R., Huang, C., Lahidji, V., Freeberg,  
1034 J., Thorner, L., Tomic, M., Separation of oxidized variants of a monoclonal antibody by anion-  
1035 exchange. *J. Chromatogr. A* 2011, 1218, 2091–2097.

1036 [120] Kaltenbrunner, O., Tauer, C., Brunner, J., Jungbauer, A., Isoprotein analysis by ion-  
1037 exchange chromatography using a linear pH gradient combined with a salt gradient. *J.*  
1038 *Chromatogr A* 1993, 639, 41–49.

1039 [121] Zhang, L., Patapoff, T., Farnan, D., Zhang, B., Improving pH gradient cation-exchange  
1040 chromatography of monoclonal antibodies by controlling ionic strength. *J. Chromatogr. A*  
1041 2013, 1272, 56–64.

1042 [122] Farnan, D., Moreno, G. T., Multiproduct high-resolution monoclonal antibody charge  
1043 variant separations by pH gradient ion-exchange chromatography. *Anal. Chem.* 2009, 81, 8846–  
1044 8857.

1045 [123] Rea, J. C., Moreno, G. T., Lou, Y., Farnan, D., Validation of a pH gradient-based ion-  
1046 exchange chromatography method for high-resolution monoclonal antibody charge variant  
1047 separations. *J. Pharm. Biomed. Anal.* 2011, 54, 317–323.

1048 [124] Kang, X., Frey, D. D., High-performance cation-exchange chromatofocusing of proteins.  
1049 *J. Chromatogr. A* 2003, 991, 117–128.

1050 [125] Vetter, T. A., Ferreira, G., Robbins, D., Carta, G., Mixed-beds of strong and weak anion  
1051 exchange resins for protein separations with step-induced pH gradients. *Sep. Sci. Techn.* 2014,  
1052 49, 477–489.

1053 [126] Vetter, T. A., Ferreira, G., Robbins, D., Carta, G., Resolution of protein charge variants  
1054 in mixed-bed chromatography columns with step-induced pH gradients at high protein  
1055 loadings. *Sep. Sci. Techn.* 2015, 50, 2211–2219.

1056 [127] Liu, Y., Anderson, D. J., Gradient chromatofocusing high-performance liquid  
1057 chromatography. I: Practical aspects. *J. Chromatogr. A* 1997, 762, 207–217.

1058 [128] Shan, L., Anderson, D. J., Effect of buffer concentration on gradient chromatofocusing  
1059 performance separating proteins on a high-performance DEAE column. *J. Chromatogr. A* 2001,  
1060 909, 191–205.

1061 [129] Shan, L., Anderson, D. J., Gradient chromatofocusing versatile pH gradient separation of  
1062 proteins in ion-exchange HPLC: characterization studies. *Anal. Chem.* 2002, 74, 5641–5649.

1063 [130] Nordborg, A., Zhang, B., He, X. Z., Hilder, E. F., Haddad, P. R., Characterization of  
1064 monoclonal antibodies using polymeric cation exchange monoliths in combination with salt  
1065 and pH gradients. *J. Sep. Sci* 2009, 32, 2668–2673.

1066 [131] Talebi, M., Nordborg, A., Gaspar, A., Lacher, N. A., Wang, Q., He, X. Z., Haddad, P. R.,  
1067 Hilder, E. F., Charge heterogeneity profiling of monoclonal antibodies using low ionic strength  
1068 ion-exchange chromatography and well-controlled pH gradients on monolithic columns. *J.*  
1069 *Chromatogr. A* 2013, 1317, 148–154.

1070 [132] Lingg, N., Tan, E., Hintersteiner, B., Bardor, M., Jungbauer, A., Highly linear pH  
1071 gradients for analyzing monoclonal antibody charge heterogeneity in the alkaline range. *J.*  
1072 *Chromatogr. A* 2013, 1319, 65–71.

1073 [133] Lin, S., Baek, J., Rao, S., Agroskin, Y., Pohl, C., Decrop, W., Milton, D., A novel pH  
1074 gradient separation platform for monoclonal antibody (MAb) charge variant analysis. Thermo  
1075 Fisher Scientific, application note 2014, 20784, 1–6.

1076 [134] Fenn, J. B., Electrospray wings for molecular elephants (Nobel Lecture). *Angew. Chem.*  
1077 *Int. Ed.* 2003, 42, 3871–3894.

1078 [135] Fenn, J. B., Mann, M., Meng, C. K., Wong, S. F., Whitehouse, C. M., Electrospray  
1079 ionization for mass spectrometry of large biomolecules. *Science* 1989, 246, 64–71.

1080 [136] Wilm, M., Mann, M., Analytical properties of the nanoelectrospray ion source. *Anal.*  
1081 *Chem.* 1996, 68, 1–8.

1082 [137] André, M., Le Caer, J.-P., Greco, C., Planchon, S., El Nemer, W., Boucheix, C.,  
1083 Rubinstein, E., Chamot-Rooke, J., Le Naour, F., Proteomic analysis of the tetraspanin web  
1084 using LC-ESI-MS/MS and MALDI-FTICR-MS. *Proteomics* 2006, 6, 1437–1449.

1085 [138] Boeri Erba, E., Petosa, C., The emerging role of native mass spectrometry in  
1086 characterizing the structure and dynamics of macromolecular complexes. *Protein Sci. Publ.*  
1087 *Protein Soc.* 2015, 24, 1176–1192.

1088 [139] Sobott, F., Robinson, C. V., Characterising electrosprayed biomolecules using tandem-  
1089 MS—the noncovalent GroEL chaperonin assembly. *Int. J. Mass Spectrom.* 2004, 236, 25–32.

1090 [140] Benesch, J. L. P., Aquilina, J. A., Ruotolo, B. T., Sobott, F., Robinson, C. V., Tandem  
1091 mass spectrometry reveals the quaternary organization of macromolecular assemblies. *Chem.*  
1092 *Biol.* 2006, 13, 597–605.

1093 [141] Heck, A. J. R., Native mass spectrometry: a bridge between interactomics and structural  
1094 biology. *Nat. Methods* 2008, 5, 927–933.

1095 [142] Leney, A. C., Heck, A. J. R., Native Mass Spectrometry: What is in the Name? *J. Am.*  
1096 *Soc. Mass Spectrom.* 2017, 28, 5–13.

1097 [143] Wohlgemuth, I., Lenz, C., Urlaub, H., Studying macromolecular complex stoichiometries  
1098 by peptide-based mass spectrometry. *Proteomics* 2015, 15, 862–879.

1099 [144] Laganowsky, A., Reading, E., Hopper, J. T. S., Robinson, C. V., Mass spectrometry of  
1100 intact membrane protein complexes. *Nat. Protoc.* 2013, 8, 639–651.



1101 [145] Berkowitz, S. A., Engen, J. R., Mazzeo, J. R., Jones, G. B., Analytical tools for  
1102 characterizing biopharmaceuticals and the implications for biosimilars. *Nat. Rev. Drug Discov.*  
1103 2012, 11, 527–540.

1104 [146] Thompson, N. J., Rosati, S., Heck, A. J. R., Performing native mass spectrometry analysis  
1105 on therapeutic antibodies. *Methods* 2014, 65, 11–17.

1106 [147] Kaltashov, I. A., Abzalimov, R. R., Do Ionic Charges in ESI MS Provide Useful  
1107 Information on Macromolecular Structure? *J. Am. Soc. Mass Spectrom.* 2008, 19, 1239–1246.

1108 [148] Gong, X., Xiong, X., Qi, L., Fang, X., Investigating the structural transitions of proteins  
1109 during dissolution by mass spectrometry. *Talanta* 2017, 164, 418–426.

1110 [149] Lanucara, F., Holman, S. W., Gray, C. J., Eyers, C. E., The power of ion mobility-mass  
1111 spectrometry for structural characterization and the study of conformational dynamics. *Nat.*  
1112 *Chem.* 2014, 6, 281–294.

1113 [150] Terral, G., Beck, A., Cianférani, S., Insights from native mass spectrometry and ion  
1114 mobility-mass spectrometry for antibody and antibody-based product characterization. *J.*  
1115 *Chromatogr. B* 2016, 1032, 79–90.

1116 [151] Rosati, S., van den Bremer, E. T., Schuurman, J., Parren, P. W., Kamerling, J. P., Heck,  
1117 A. J., In-depth qualitative and quantitative analysis of composite glycosylation profiles and  
1118 other micro-heterogeneity on intact monoclonal antibodies by high-resolution native mass  
1119 spectrometry using a modified Orbitrap. *mAbs* 2013, 5, 917–924.

1120 [152] Hernández, H., Robinson, C. V., Determining the stoichiometry and interactions of  
1121 macromolecular assemblies from mass spectrometry. *Nat. Protoc.* 2007, 2, 715–726.

1122 [153] Sterling, H. J., Batchelor, J. D., Wemmer, D. E., Williams, E. R., Effects of buffer loading  
1123 for electrospray ionization mass spectrometry of a noncovalent protein complex that requires  
1124 high concentrations of essential salts. *J. Am. Soc. Mass Spectrom.* 2010, 21, 1045–1049.

1125 [154] Xiu, L., Valeja, S. G., Alpert, A. J., Jin, S., Ge, Y., Effective protein separation by  
1126 coupling hydrophobic interaction and reverse phase chromatography for top-down proteomics.  
1127 *Anal. Chem.* 2014, 86, 7899–7906.

1128 [155] Chen, B., Peng, Y., Valeja, S. G., Xiu, L., Alpert, A. J., Ge, Y., Online hydrophobic  
1129 interaction chromatography–mass spectrometry for top-down proteomics. *Anal. Chem.* 2016,  
1130 88, 1885–1891.

1131 [156] Rose, R. J., Damoc, E., Denisov, E., Makarov, A., Heck, A. J. R., High-sensitivity  
1132 Orbitrap mass analysis of intact macromolecular assemblies. *Nat. Methods* 2012, 9, 1084–1086.

1133 [157] Tito, M. A., Miller, J., Walker, N., Griffin, K. F., Williamson, E. D., Despeyroux-Hill,  
1134 D., Titball, R. W., Robinson, C. V., Probing molecular interactions in intact antibody: antigen  
1135 complexes, an electrospray time-of-flight mass spectrometry approach. *Biophys. J.* 2001, 81,  
1136 3503–3509.

1137 [158] Maggi, A., Ruivo, E., Fissers, J., Vangestel, C., Chatterjee, S., Joossens, J., Sobott, F.,  
1138 Staelens, S., Stroobants, S., Veken, P. V. D., Wyffels, L., Augustyns, K., Development of a  
1139 novel antibody–tetrazine conjugate for bioorthogonal pretargeting. *Org. Biomol. Chem.* 2016,  
1140 14, 7544–7551

1141 [159] Valliere-Douglass, J. F., McFee, W. A., Salas-Solano, O., Native intact mass  
1142 determination of antibodies conjugated with monomethyl auristatin E and F at interchain  
1143 cysteine residues. *Anal. Chem.* 2012, 84, 2843–2849.

1144 [160] Debaene, F., Boeuf, A., Wagner-Rousset, E., Colas, O., Ayoub, D., Corvaia, N., Van  
1145 Dorsselaer, A., Beck, A., Cianfèrani, S., Innovative native MS methodologies for antibody drug  
1146 conjugate characterization: High resolution native MS and IM-MS for average DAR and DAR  
1147 distribution assessment. *Anal. Chem.* 2014, 86, 10674–10683.

1148

**Table I.** Overview of SEC columns applied for the separation therapeutic proteins frequently reported in scientific literature.

Column	Matrix	Chemistry	Particle size ( $\mu\text{m}$ )	Pore size ( $\text{\AA}$ )	pH stability	Max Pressure (MPa)	Brand
Advanced Bio SEC	Silica	Silanol	2.7	300	2-8.5	10	Agilent Technologies
Yarra SEC-X300	Silica	Silanol	1.8	300	1.5-8.5	48	Phenomenex
Unix-C SEC 300	Silica	Diol	1.8	300	2-8.5	31	Sepax Technologies
Zenix SEC-300	Silica	Diol	3	300	2-8.5	7	Sepax Technologies
MABPac SEC 1	Silica	Diol	5	300	2-7.5	7	Thermo Fisher Scientific
TSKgel SuperSW mAb HR	Silica	Diol	4	250	2-7.5	8	Tosoh Bioscience
TSKgel UltraSW Aggregate	Silica	Diol	3	3000	2-7.5	12	Tosoh Bioscience
Protein-Pak SEC	Silica	Diol	10	300	2-8	30	Waters
XBridge Protein BEH SEC	Silica	Silanol	3.5	200	1-8	Not available	Waters

**Table II.** Overview of HIC columns applied for the separation therapeutic proteins frequently reported in scientific literature.

Column	Matrix	Chemistry	Particle size ( $\mu\text{m}$ )	Pore size ( $\text{\AA}$ )	pH stability	Max Pressure (MPa)	Brand
Proteomix HIC 1.7	PS/DVB	Butyl/Ethyl	1.7	Non porous	2-12	50	Sepax Technologies
Proteomix HIC 5	PS/DVB	Phenyl/Butyl/ Propyl/Ethyl	5	Non porous	2-12	41	Sepax Technologies
MABPAc HIC-10	Silica	Alkyl amide	5	1000	2-8	55	Thermo Fisher Scientific
MABPAc HIC-20	Silica	Alkyl amide	5	1000	2-9	55	Thermo Fisher Scientific
MABPAc HIC-Butyl	Polymer	Poly amide	5	Non porous	2-12	27	Thermo Fisher Scientific
TSKgel Butyl-NPR	Polymethacrylate	Butyl	2.5	Non porous	2-12	20	Tosoh Bioscience
TSKgel Phenyl-5PW	Polymethacrylate	Ether	13, 10	1000	2-12	2	Tosoh Bioscience
TSKgel Ether-5PW	Polymethacrylate	Polyamine	10	1000	2-12	2	Tosoh Bioscience
Protein-Pak Hi Res HIC	Polymethacrylate	Ether	10	Non porous	2-12	20	Waters

**Table III.** Overview of IEX columns applied for the separation therapeutic proteins frequently reported in scientific literature.

Column	Matrix	Chemistry	Particle size ( $\mu\text{m}$ )	Pore size ( $\text{\AA}$ )	pH stability	Max Pressure (MPa)	Brand
Agilent Bio SCX	PS/DVB	Sulfonic acid	10, 5, 3, 1.7	Non porous	2-12	68	Agilent Technologies
WP CBX	Silica	Sulfonic acid	5	300	2-8	45	Avantor Inc
Antibodix WCX	PS/DVB	Carboxylate	10, 5, 3, 1.7	Non porous	2-12	68	Sepax Technologies
Proteomix SCX	PS/DVB	Sulfonic acid	10, 5, 3, 1.7	Non porous	2-12	68	Sepax Technologies
BioBasic SCX LC	Silica	Sulfonic acid	5	300	2-8	40	Thermo Fisher Scientific
MabPac SCX	Polymer	Sulfonic acid	10	Non porous	2-12	20	Thermo Fisher Scientific
TSKgel Q-STAT	Polymer	Quaternary ammonium	10	Non porous	3-10	5	Tosoh Bioscience
TSKgel Bioassist Q	Polymethacrylate	Polyamine	13, 10	4000	2-12	2	Tosoh Bioscience
Protein-Pak HiRes CM	Polymethacrylate	Carboxymethyl	7	Non porous	3-10	15	Waters

1 **Figure captions**

2 **Figure 1.** SEC analysis of a Protein A purified monoclonal antibody recombinantly expressed in  
3 Chinese Hamster Ovarian (CHO) cells performed on a 7.84.0 mm i.d. × 300 mm long AdvanceBio  
4 SEC column packed with 2.7 μm particles containing 300Å pores. Separation conducted applying  
5 a mobile phase of 150 mM sodium phosphate pH 7, a flow rate of 0.8 mL/min, and UV detection  
6 at 220 nm.

7

8 **Figure 2.** Overlay of selected SEC chromatograms extracted from over 1500 injections of  
9 bevacizumab performed on a 4.0 mm i.d. × 300 mm long MAbPac SEC-1 column packed with 5  
10 μm macroporous particles applying 100 mM sodium phosphate pH 6.8 in 300 mM NaCl as the  
11 mobile phase. Adapted with permission from [58].

12

13 **Figure 3.** HIC separation of ADCs having different payload in which the retention time increases  
14 with increasing DAR. Adapted with permission from [82].

15

16 **Figure 4.** Optimization of an E. coli acetone powders separation in anion-exchange mode by A) a  
17 salt gradient with decreasing the slope of the NaCl salt gradient in time, and by B) application of  
18 a pH gradient; decreasing the slope of the pH-gradient in the range between pH 3.5-2.4. C) shows  
19 the respective salt and pH gradient profiles. For the salt gradients, a 20 mM sodium carbonate  
20 buffer at pH 9.7 was used as mobile-phase A and 20 mM sodium carbonate buffer at pH 9.7  
21 containing 1 mM NaCl was used as mobile-phase B. For the pH gradients, a proprietary pISep  
22 buffer (mixture of polyionic organic buffering molecules) at pH 2.4 was used as buffer A, and

23 buffer B consisted of pISep buffer at pH 10.9. The column volume (CV) was approximately 2  
24 mL. The applied gradient slopes are:  $a_1$ : 13.6 mM NaCl/CV,  $a_2$ : 10.9 mM NaCl/CV,  $a_3$ : 8.0 mM  
25 NaCl/CV,  $a_4$ : 5.0 mM NaCl/CV,  $a_5$ : 4.3 mM NaCl/CV for the salt-gradient profiles, and  $b_1$  and  $b_2$ :  
26 0.1 pH units/CV,  $b_3$ : 0.1 pH units/CV from pH 9.7-3.5 and 0.05 pH units/CV from pH 3.5-2.4,  $b_4$ :  
27 0.1 pH units/CV from pH 9.7-3.5 and 0.025 pH units/CV from pH 3.5-2.4 for the pH-gradient  
28 profiles. Adapted with permission from [107].

29

30 **Figure 5.** Schematic overview of the different state encountered in protein MS analysis.

31

32 **Figure 6.** ESI mass spectra of anti-thrombin III (A) acquired under native MS conditions using 20  
33 mM ammonium acetate, (B) using 20 mM ammonium acetate/methanol/formic acid 49:50:5  
34 (v/v/v)%, and (C) denaturing conditions using 20 mM ammonium acetate/methanol/formic acid  
35 45:50:5 (v/v/v)%. Adapted with permission from [147].

36

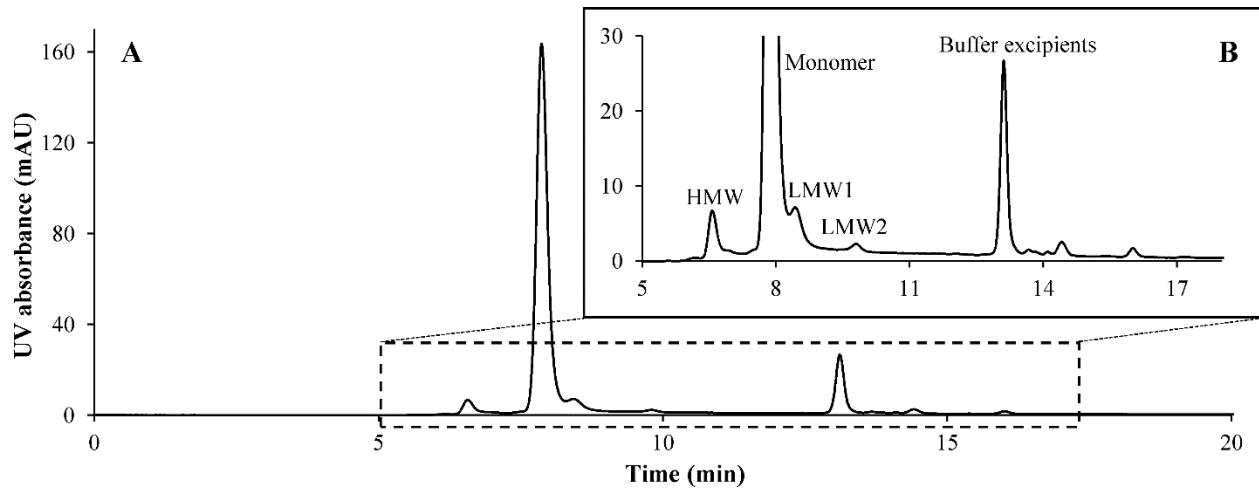
37 **Figure 7.** (A) Native MS spectrum of a deglycosylated mAb (IgG1) yielding a narrow charge  
38 envelope situated in the high  $m/z$  region and corresponding deconvoluted mass spectrum shown  
39 in the inset to determine the intact mass. (B) Subsection of a native MS spectrum from a  
40 glycosylated mAb displaying increased mass heterogeneity and corresponding deconvoluted mass  
41 spectrum in the inset revealing the presence of different glycoforms. Adapted with permission  
42 from [146].

43

44 **Figure 8.** Native MS spectra of IgGs (CNTO5825 and NIST) obtained on a Q-TOF-2 instrument  
45 (Waters) after direct infusion (A and B) and after SEC analysis, indicating partial unfolding of the  
46 antibodies (without breaking disulfide bonds). LC conditions: Flow rate = 0.1 mL/min; mobile  
47 phase = 100 mM ammonium acetate, pH 6.8; using a 4.6 mm i.d. × 100 mm BEH SEC column  
48 packed with 1.7 μm particles (200Å pores).

49

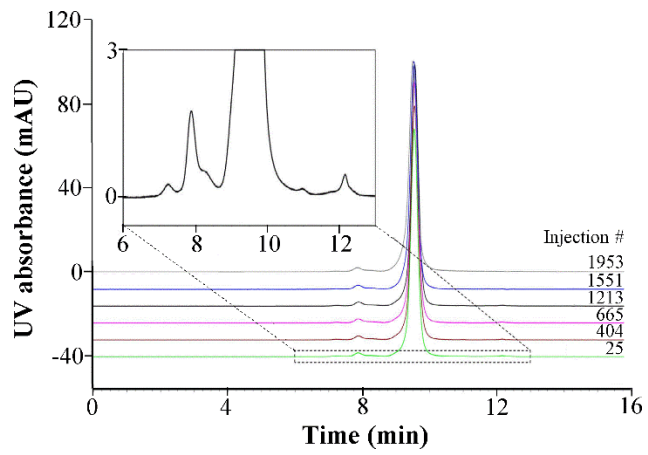




50

51 Figure 1

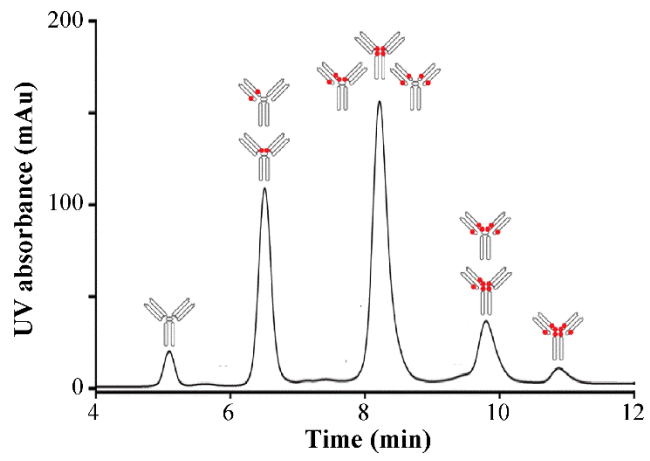
52



53

54 Figure 2

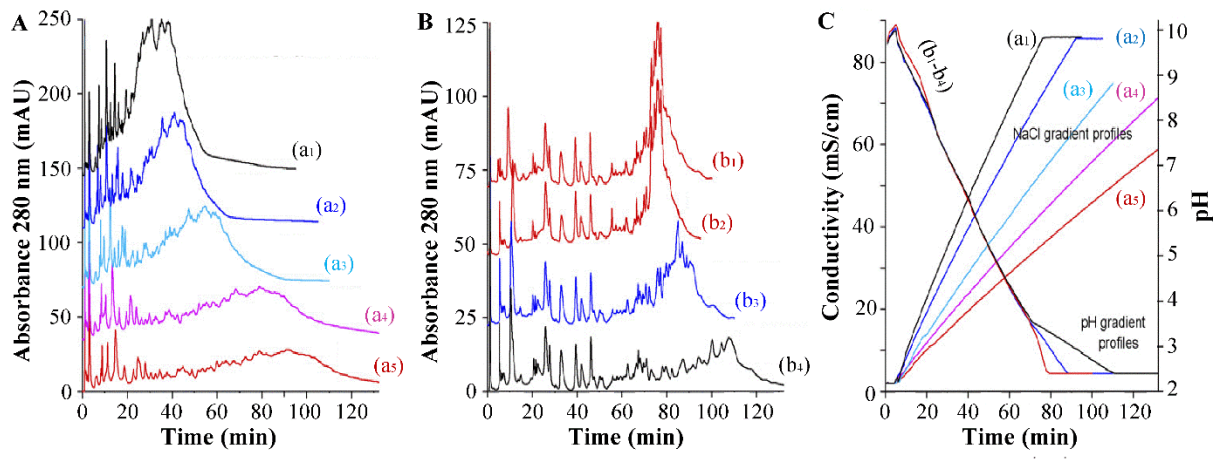
55



56

57 Figure 3

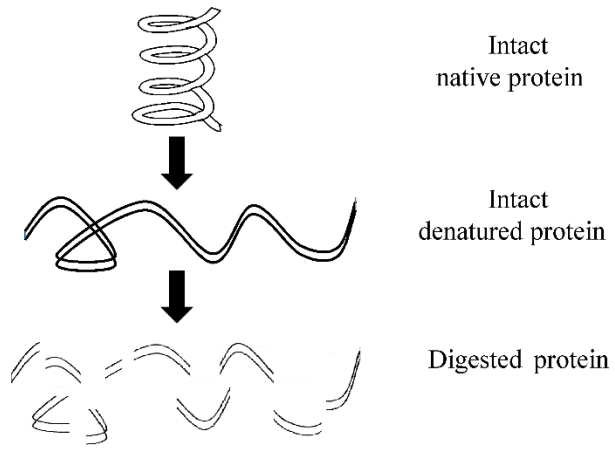
58



59

60 Figure 4

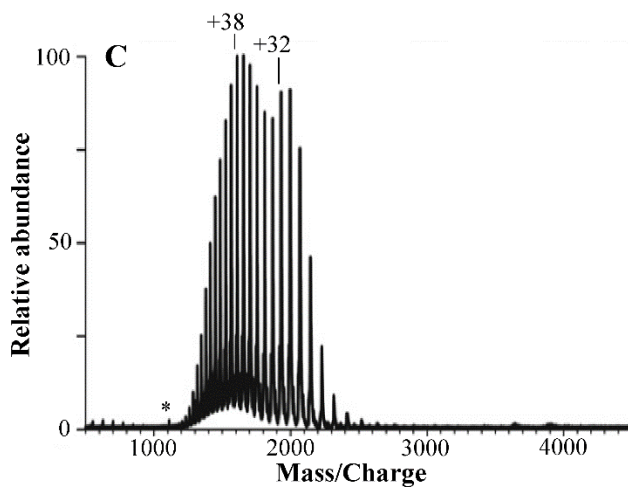
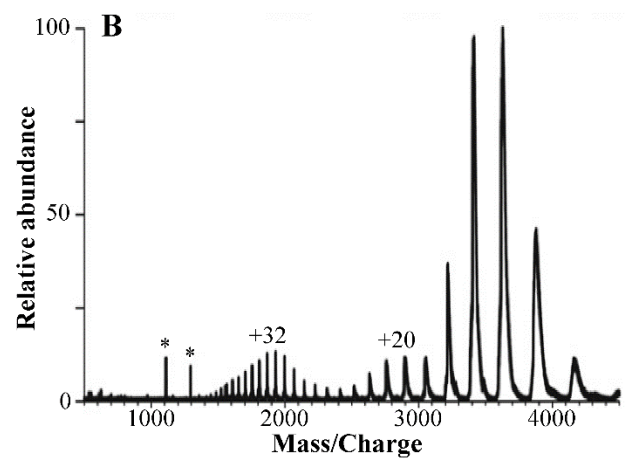
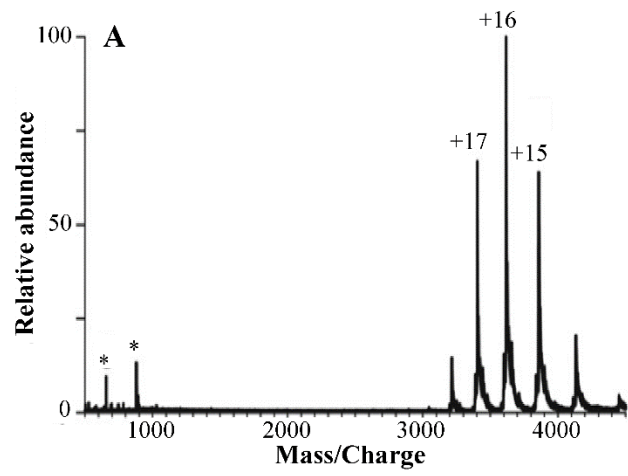
61



62

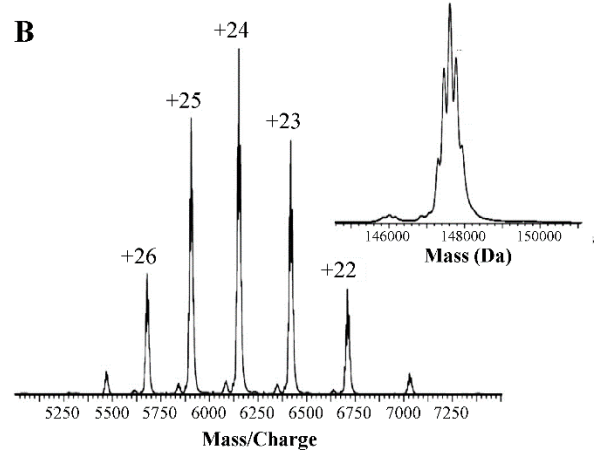
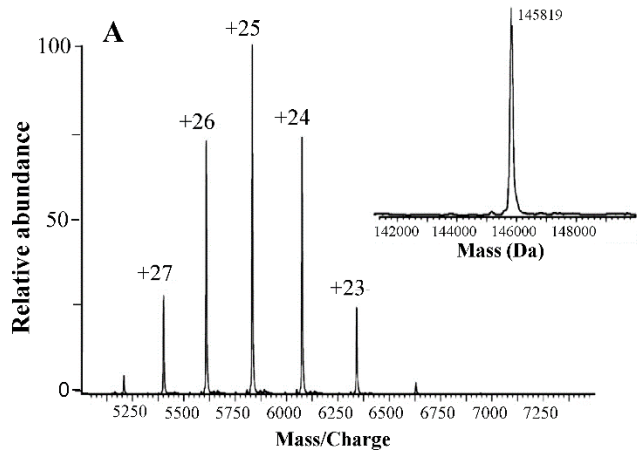
63 Figure 5

64



65

66 Figure 6



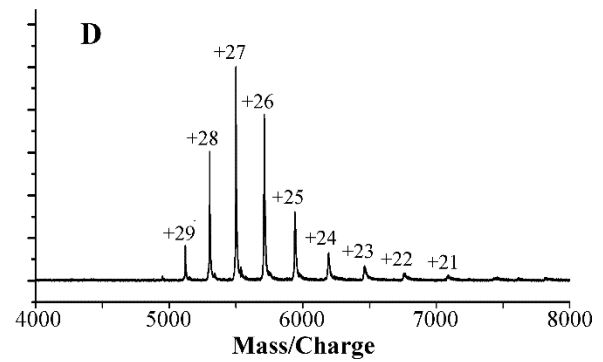
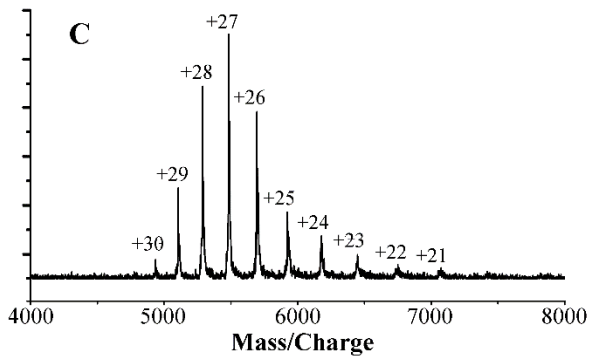
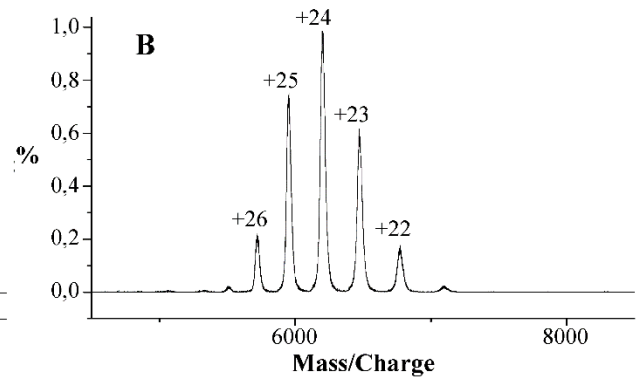
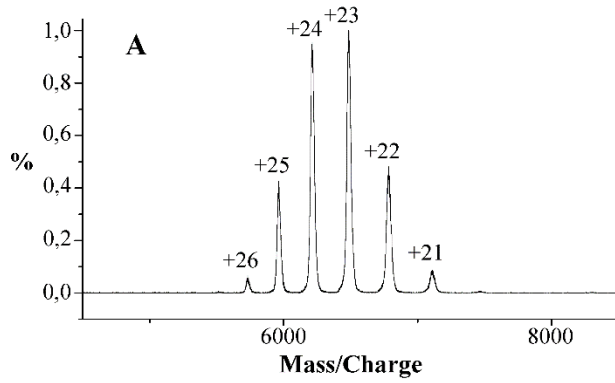
67

68 Figure 7

69

### CNT05825

### NIST IgG1



70

71 Figure 8